A hybrid metaheuristic for the electric vehicle routing problem with partial charging and nonlinear charging function

Alejandro Montoya, Christelle Guéret, Jorge E. Mendoza, Juan G. Villegas

A hybrid metaheuristic for the electric vehicle routing problem with nonlinear charging function

Alejandro Montoya[a,b], Christelle Guéret[a], Jorge E. Mendoza[c], Juan G. Villegas[d,*]

[a]*Université d'Angers, LARIS (EA 7315), 62 avenue Notre Dame du Lac, 49000 Angers, France*
[b]*Departamento de Ingeniería de Producción, Universidad EAFIT, Carrera 49 No. 7 Sur - 50, Medellín, Colombia*
[c]*Université François-Rabelais de Tours, CNRS, LI (EA 6300), OC (ERL CNRS 6305), 64 avenue Jean Portalis, 37200 Tours, France*
[d]*Departamento de Ingeniería Industrial, Facultad de Ingeniería, Universidad de Antioquia, Calle 70 No. 52-21, Medellín, Colombia*

Abstract

In this paper we consider the electric vehicle routing problem with nonlinear charging function (eVRP-NL), a variant of the electric vehicle routing problem with more-realistic assumptions about the battery charging process. To tackle the problem, we propose an iterated local search (ILS) enhanced with heuristic concentration (HC). At each iteration, our ILS applies a variable neighborhood descent (VND) procedure with three different local search operators and stores the routes of the local optimum in a pool of routes. When the ILS finishes, the HC component assembles the final solution by recombining routes from the pool. One original feature of our approach is the use in the VND component of a local search operator that aims at improving the charging decisions of each route (where and how much to charge). To achieve this goal, the operator solves a new optimization problem: the fixed-route vehicle-charging problem (FRVCP). Our implementation solves the FRVCP using a heuristic and a commercial solver. To test our approach, we propose a new 120-instance testbed for the e-VRP-PNL. We discuss experiments assessing the performance of the proposed approach and showing the relevance of making optimal charging decisions.

Keywords: Vehicle routing problem, Electric vehicle routing problem with nonlinear charging function, Iterated local search (ILS), Matheuristic

1. Introduction

Electric vehicles (EVs) are a promising technology for reducing greenhouse gas emissions and transportation costs in goods distribution (Electrification-Coalition 2013, TU Delft

---

*Corresponding author
Email addresses: `jmonto36@eafit.edu.co` (Alejandro Montoya),
`christelle.gueret@univ-angers.fr` (Christelle Guéret), `jorge.mendoza@univ-tours.fr` (Jorge E. Mendoza), `juan.villegas@udea.edu.co` (Juan G. Villegas)

2013). Therefore, it is not surprising that every day more companies add EVs to their fleets. Probably the two earliest successful implementations were those reported by La Poste (Kleindorfer et al. 2012) and UPS (UPS 2008). Since then, several companies of different sectors and sizes have started to use EVs (Nesterova et al. 2015). For instance: the Portuguese postal company CTT operates with 10 small electric vans (Post & Parcel 2014); Heineken uses Europe's larges fleet of EVs to distribute beer in Amsterdam (Heineken 2013); Bimbo, the largest F&B company in Mexico, signed orders to buy 100 EVs which will use the energy from a wind farm (Ramirez 2015); and in Colombia a health care company uses EVs for their home healthcare service (Loaiza 2014).

The use of EVs in goods distribution and services introduces a new family of vehicle routing problems (VRPs), the so-called electric VRPs (eVRPs) (Pelletier et al. 2016). These problems extend classical VRPs to consider the limited driving range of EVs and their long battery charging times. Because of the short driving range, eVRP solutions frequently include routes with planned detours to charging stations (CSs) where the EVs recharge. In general, eVRP models make assumptions about the capacity of the CSs, the EV energy consumption, and the EV battery charging process. This research focuses on the latter.

To model the battery charging process, eVRP models make assumptions about the *charging policy* and the *charging function approximation*. The former defines how much of the battery capacity can be (or must be) restored when an EV visits a CS, and the latter models the relationship between battery charging time and charging level. With respect to the charging policies, the eVRP literature can be classified into two groups: studies assuming *full* and *partial* charging policies. As the name suggests, in full charging policies, the battery capacity is fully restored every time an EV reaches a CS. Some studies in this group assume that there is no charging function but rather a constant charging time (Conrad & Figliozzi 2011, Erdoğan & Miller-Hooks 2012, Montoya et al. 2015). This is a plausible assumption in applications where the CSs replace a (partially) depleted battery with a fully charged one. On the other hand, Schneider et al. (2014), Hiermann et al. (2016), Desaulniers et al. (2014), Goeke & Schneider (2015), Schneider et al. (2015), and Szeto & Cheng (2016) consider full charging policies with a linear charging function approximation (i.e., the battery level is assumed to be a linear function of the charging time). In their models, the time spent at each CS depends on the battery level when the EV arrives and on the (constant) charging rate of the CS. In partial charging policies, the amount of charge (and thus the time spent at each charging point) is a decision variable. To the best of our knowledge, all existing eVRP models with partial charging consider linear function approximations (Felipe et al. 2014, Desaulniers et al. 2014, Sassi et al. 2015, Bruglieri et al. 2015, Schiffer & Walther 2015, Keskin & Çatay 2016).

In practice, using linear approximations to model the charging function may not be pertinent. Indeed, it is well documented that the charging level is a concave function of the charging time (Bruglieri et al. 2014, Hõimoja et al. 2012, Pelletier et al. 2015). To assess the impact of neglecting the nonlinear nature of the charging function, we conducted a study comparing optimal solutions found under different battery charging assumptions commonly used in the literature. The results of the study show that solutions found under the linear approximation assumption may turn out to be infeasible or overly expensive in practice.

This study can be found in the supplementary material of this paper.

The main contributions of this research are fourfold. First, we introduce the electric vehicle routing problem with nonlinear charging functions (eVRP-NL), a new eVRP that considers more realistic assumptions about the charging process. Second, we introduce and study a new variant of the fixed-route vehicle-charging problem (FRVCP) that appears as a subproblem of the eVRP-NL. The FRVCP consists in finding the optimal charging decisions (i.e., where and how much to charge) for a route servicing a fixed sequence of customers. Third, we propose a hybrid metaheuristic to solve the eVRP-NL and assess its performance in a new set of benchmark instances. Fourth, analyze our solutions and provide some insight into the characteristics of good eVRP-NL solutions.

The remainder of this paper is organized as follows. Section 2 describes the problem. Section 3 introduces our hybrid metaheuristic. Section 4 discusses the FRVCP and presents two approaches to solve it. Section 5 presents a computational evaluation of the proposed method. Finally, Section 6 concludes the paper and outlines future work.

2. Problem description

Formally, the eVRP-NL can be defined on a directed and complete graph $G = (V, A)$. The vertex set $V = \{0\} \cup I \cup F$ is made up of a depot (vertex 0), a set of customers I, and a set of CSs F. Each customer $i \in I$ has a service time p_i. Each CS $i \in F$ has a nonlinear charging function, which is modeled using a piecewise linear approximation. This approximation is defined by a set of breakpoints B, where each breakpoint $k \in B$ is associated to a charging time c_{ik} and a charge level a_{ik} (see Figure 1). The set $A = \{(i, j) : i, j \in V, i \neq j\}$ corresponds to arcs connecting vertices in V. Each arc (i, j) has two associated nonnegative values: a travel time t_{ij} and an energy consumption e_{ij}. The customers are served using an unlimited and homogeneous fleet of EVs. All the EVs have a battery of capacity Q (expressed in kWh) and a maximum tour duration T_{max}. It is assumed that the EVs leave the depot with a fully charged battery, and that all the CSs can handle an unlimited number of EVs simultaneously. Feasible solutions to the eVRP-NL satisfy the following conditions: each customer is visited exactly once; each route satisfies the maximum-duration limit; each route starts and ends at the depot; and the battery level when an EV arrives to and departs from any vertex is between 0 and Q.

Since the distance is directly related to the energy consumption, most work on eVRPs with homogeneous fleet focuses on minimizing the total distance (Schneider et al. 2014, Desaulniers et al. 2014, Hiermann et al. 2016, Keskin & Çatay 2016). However, this objective function neglects the impact of charging operations in the cost of the solutions. This may lead to decisions such as: charging the batteries more than needed, or charging the batteries when their level is high. These decisions directly affect the battery's long-term degradation cost (which according to Becker et al. (2009) can be threefold the energy cost) and the charging fees at CSs (Bansal 2015). To better capture the impact of charging operations, in the eVRP-NL we minimize the total travel and charging time. This objective function has been studied by Zündorf (2014) and Liao et al. (2016) on related routing problems.
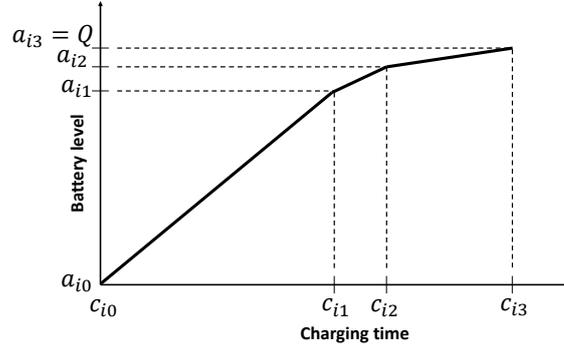
Figure 1: Piecewise linear approximation composed of 3 linear segments for a CS of $22\,\text{kW}$ of power, charging a battery with $Q = 16\,\text{kWh}$.

Figure 2 presents a numerical example illustrating the eVRP-NL. The figure depicts a solution to an instance with 7 customers and 3 CSs. The CSs have different technologies (slow and fast), and each technology has a particular piecewise-linear charging function. In the charging functions, variables q_i and o_i specify the battery levels when an EV arrives at and departs from CS $i \in F$. The charging function maps these variables to charging times s_i and e_i, in order to estimate the time spent at the CS (Δ_i). In this example, Route 1 does not visit any CS, because its total energy consumption is less than the battery capacity. On the other hand Route 2 visits CS 8. In this route, the EV arrives at the CS with a battery level $q_8 = 1.0$, and it charges the battery to a level $o_8 = 6.0$. To estimate the time spent at the CS, we use the piecewise-linear charging function: the charging time associated to q_8 and o_8 are $s_i = 0.8$ and $e_i = 6.0$, then the time spent at CS 8 is $\Delta_8 = 6.0 - 0.8 = 5.2$. The duration of Route 2 is the sum of the travel time (13.0), the charging time (5.2), and the service time (1.0), that is, 19.2 which is lower than $Tmax$. The cost of this route is 18.2 (travel time + charging time). Finally, Route 3 visits CSs 10 and 9; and it spends $\Delta_{10} = 7.2$ and $\Delta_9 = 1.6$ time units charging in these CSs, respectively. In addition to the problem description and numerical example, to help the reader understanding the eVRP-NL, we have included a mixed integer linear programming (MILP) formulation of the problem in the supplementary material.
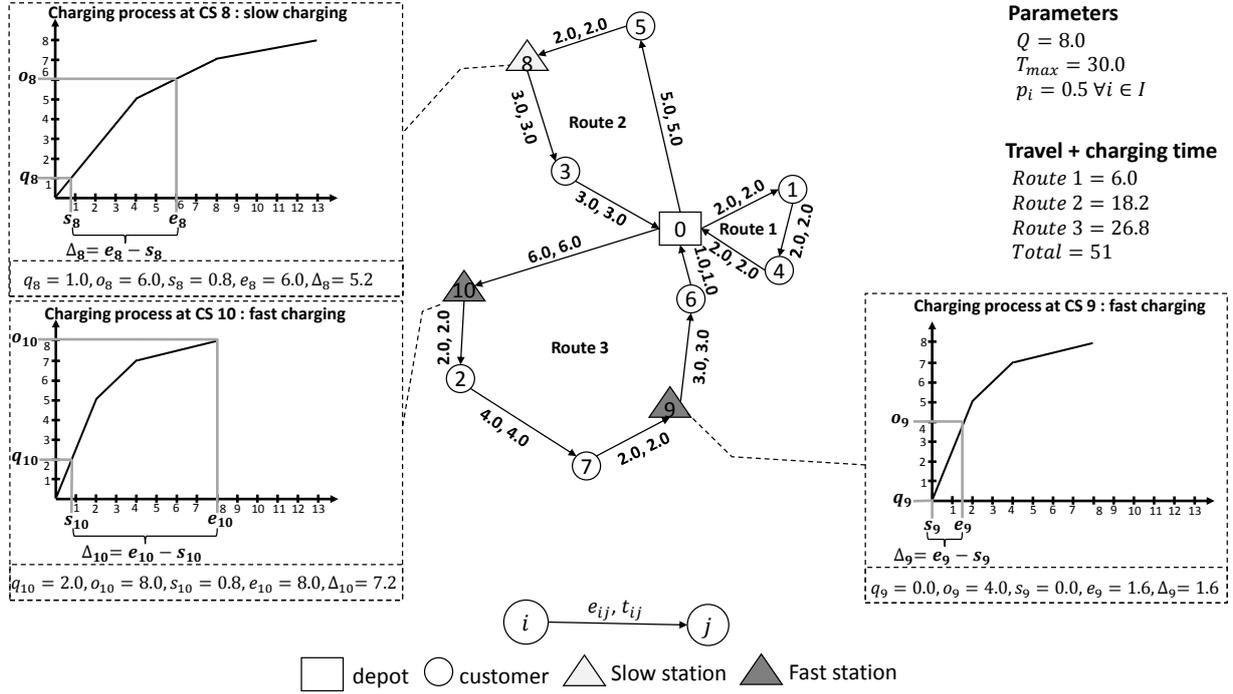
Figure 2: Example of a feasible eVRP-NL solution

3. Hybrid metaheuristic

To solve the eVRP-NL we developed a hybrid metaheuristic combining ILS (Lourenço et al. 2010) an HC (Rosing & ReVelle 1997). Figure 3 presents the general structure of the proposed approach (hereafter referred to as ILS+HC).

To find an initial solution we follow a sequence-first split-second approach which uses a constructive heuristic to build a TSP tour visiting all the customers and a splitting procedure to retrieve an eVRP-NL solution. Then, at each iteration of the ILS we improve the current solution using a variable neighborhood descent (VND) (Mladenović & Hansen 1997) with three local search operators: relocate, 2-Opt, and global charging improvement (GCI). At the end of each ILS iteration, we update the best solution and add the routes of the local optimum to a pool of routes Ω. To diversify the search, we concatenate the routes of the local optimum to build a new TSP tour, and then perturb the new TSP tour. We start a new ILS iteration by splitting the perturbed TSP tour. After K iterations the ILS component stops, and we carry out the HC. In this phase, we solve a set partitioning problem over the set of routes Ω to obtain an eVRP-NL solution. In the remainder of this section, we describe the main components of our method.

5
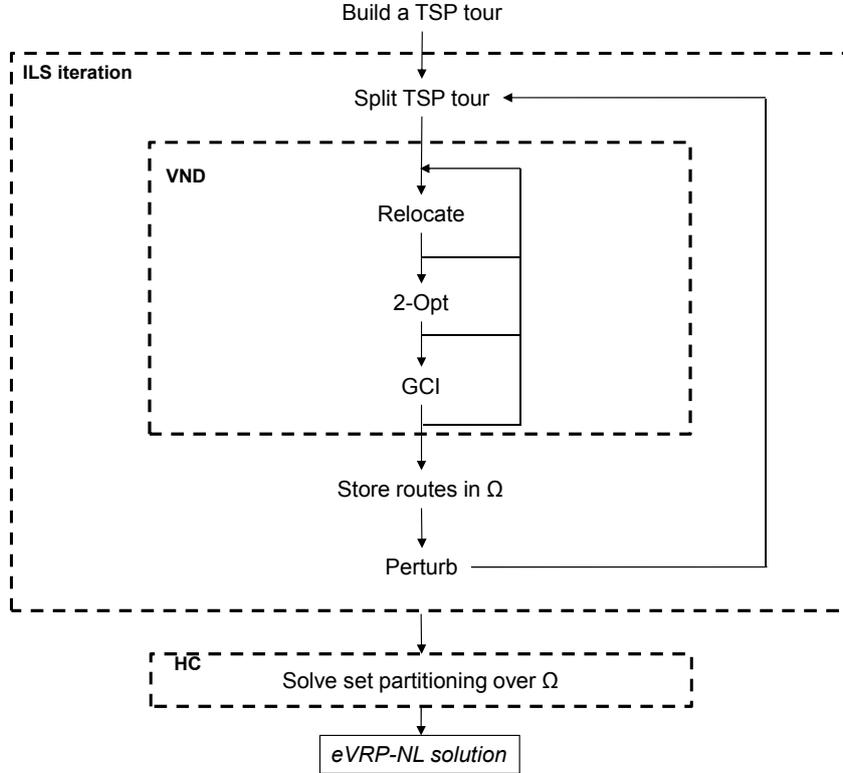
Figure 3: General structure of ILS+HC

3.1. Initial solution

We generate the initial TSP tour using the simple and well-known nearest neighbor heuristic (NN). For a description of NN see Rosenkrantz et al. (1974)

3.2. Split

To extract a feasible solution from a TSP tour, our approach uses an adaptation of the splitting procedure introduced by Prins (2004). The splitting procedure builds a directed acyclic graph $G^* = (V^*, A^*)$ composed of the ordered vertex set $V^* = (v_0, v_1, ..., v_i, ..., v_n)$ and the arc set A^*. Vertex $v_0 = 0$ is an auxiliary vertex, and each vertex v_i represents the customer in the ith position of the TSP tour. Arc $(v_i, v_{i+n_r}) \in A^*$ represents a feasible route $r_{v_i, v_{i+n_r}}$ with an energy consumption $e_{r_{v_i, v_{i+n_r}}}$, starting and ending at the depot and visiting customers in the sequence v_{i+1} to v_{i+n_r}.

Note that since the TSP tour only includes customers, route $r_{v_i, v_{i+n_r}}$ may be *energy-infeasible* (i.e., the total energy needed to cover the route is greater than Q). In that case, we solve a FRVCP to obtain an *energy-feasible* route by inserting visits to CSs. If visiting

6

CSs increases the duration of the route beyond T_{max}, we do not include the arc associated with the route in A^*. Finally, to obtain a feasible eVRP-NL solution, the splitting procedure finds the set of arcs (i.e., routes) along the shortest path connecting 0 and v_n in G^*.

3.3. Variable neighborhood descent

To improve the solution generated by the splitting procedure we use a VND based on three local search operators. The first two operators, namely, relocate and 2-Opt[1], focus on the customer sequencing decisions. In other words, these two operators only alter the sequence of customers and do not have the ability to insert, remove, or change the position of CSs. To update the charging times after a relocate or 2-Opt move we use the rule proposed by Felipe et al. (2014): when visiting a CS, charge the strict minimum amount of energy needed to continue the route until reaching the next CS (or the depot if there is no other CS downstream). If reaching the next CS (or the depot) is impossible, even with a fully charged battery, the move is deemed infeasible. Similarly, if after updating the charging times the resulting route is infeasible in terms of the maximum-duration limit, the move is simply discarded. It is worth nothing that the Felipe et al. (2014) rule is optimal when all CSs are homogeneous; nonetheless, that is not the case in our eVRP-NL.

As its name suggest, the third operator, global charging improvement or GCI, focuses on the charging decisions. GCI is applied to every route visiting at least one CS. The operator works as follows. First, GCI removes from the route all visits to CSs. If the resulting route is energy-feasible, the operator stops. On the other hand, if the route is energy-infeasible, GCI solves a FRVCP trying to optimize the charging decisions (where and how much to charge) for the concerned route. Depending on the configuration, our ILS+HC solves the underlying FRVCP either heuristically or optimally. Full details on the FRVCP and the solution techniques embedded in our approach to solve it are given in Section 4.

3.4. Perturb

To diversify the search our approach concatenates the routes of the current best solution to build a TSP tour. Then, we perturb the resulting TSP tour with a randomized double bridge operator (Lourenço et al. 2010) and then apply the split procedure to obtain a new eVRP-NL solution.

3.5. Heuristic concentration

Finally, the heuristic concentration component solves a set partitioning formulation over the pool of routes Ω. The objective is then to select the best subset of routes from Ω to build the final solution guaranteeing that each customer is visited by exactly one route.

---

[1]In our implementation we use intra-route and inter-route versions with best-improvement selection.

4. The fixed-route vehicle-charging problem

As mentioned above our ILS+HC relies on solving a variant of the FRVCP at two specific points of its execution: when evaluating routes in the split procedure, and when searching the GCI neighborhood. The FRVCP is a variant of the well-known fixed-route vehicle-refueling problem (FRVRP). The FRVRP seeks the minimum-cost refueling policy (which fuel stations to visit and the refueling quantity at each visited station) for a given origin-destination route (Suzuki 2014). Most of the research carried on the FRVRP and its variants applies only to internal combustion vehicles (which have negligible refueling times). Nonetheless, a few FRVCP variants have received attention in the literature. Most of these variants assume full charging policies (Montoya et al. 2015, Hiermann et al. 2016, Liao et al. 2016). To our knowledge, only Sweda et al. (2016) assume a partial charging policy. Their problem differs from ours in three fundamental ways: i) they do not take into account the charging times (because their objective is to minimize the energy and degradation costs), ii) they do not deal with maximum route duration constraints, and iii) in their problem the CSs are already included in the fixed route and no detours are to be planned. In the remainder of this section we introduce our FRVCP and the techniques embedded in our approach to solve it. For the sake of simplicity, in the remainder of the manuscript to refer to our FRVCP variant simply as the FRVCP.

Let $\Pi = \{\pi(0), \pi(1), ..., \pi(i), ..., \pi(j), ..., \pi(n_r)\}$ be an energy-infeasible route, where $\pi(0)$ and $\pi(n_r)$ represent the depot. The route has a total time $\bar{t}$, which is the sum of the travel times plus the service times. The feasibility of Π may be restored by inserting visits to CSs. As mentioned in Section 2, each CS $j \in F$ has a piecewise-linear charging function defined by a set of breakpoints B. The piecewise linear function is composed by a set of segments. Each segment is defined between the breakpoints $k-1$ and $k \in B$, it has a slope ρ_{jk} (representing a charging rate), and it is bounded between the battery levels a_{jk-1} and a_{jk} (see Figure 4a). Figure 4b shows the fixed-route Π and the possible visits to the CSs between two vertices of Π. In Figure 4b the values $e_{\pi(i-1)\pi(i)}$ and $t_{\pi(i-1)\pi(i)}$ represent the energy consumption and the travel time between vertices $\pi(i-1)$ and $\pi(i) \in \Pi$. Similarly, $e_{\pi(i-1)j}$ and $t_{\pi(i-1)j}$ represent the energy consumption and the travel time between vertex $\pi(i-1) \in \Pi$ and CS $j \in F$, and $e_{j\pi(i)}$ and $t_{j\pi(i)}$ represent the energy consumption and the travel time between the CS $j \in F$ and vertex $\pi(i) \in \Pi$.

In the FRVCP the objective is to find the charging decisions (where and how much to charge) that minimize the sum of the charging times and detour times while satisfying the following conditions: the level of the battery when the EV arrives at any vertex is nonnegative; the charge in the battery does not exceed its capacity; and the route satisfies the maximum-duration limit. Since the FRVRP is NP-hard (Suzuki 2014) and the FRVCP generalizes the FRVRP, we can conclude that the FRVCP is also NP-hard.

4.1. Mixed-integer linear programming formulation

We formulate the FRVCP using the following decision variables: variable $\varepsilon_{\pi(i)j}$ is equal to 1 if the EV charges at CS $j \in F$ before visiting vertex $\pi(i) \in \Pi$. Variable $\phi_{\pi(i)}$ tracks the battery level. If $\varepsilon_{\pi(i)j} = 0$, $\phi_{\pi(i)}$ is the battery level when the EV arrives at vertex $\pi(i)$. On
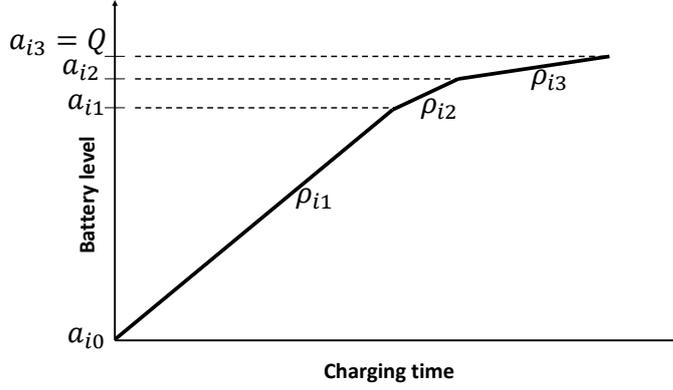
(a) Segments of the piecewise-linear charging function
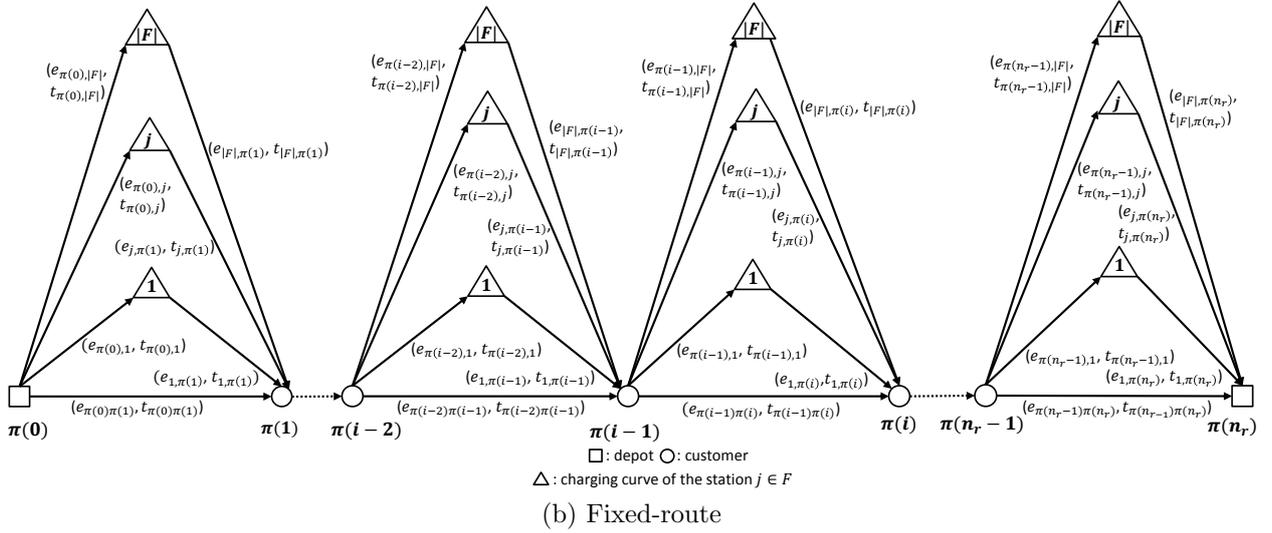
(b) Fixed-route

Figure 4: Piecewise-linear charging function and fixed-route for the FRVCP

the other hand, if $\varepsilon_{\pi(i)j} = 1$, $\phi_{\pi(i)}$ is the battery level when the EV arrives at CS $j \in F$ right before visiting vertex $\pi(i)$. Variable $\theta_{\pi(i)jk}$ is equal to 1 if the EV charges on the segment defined by breakpoints $k-1$ and $k \in B$ at CS $j \in F$ before visiting vertex $\pi(i) \in \Pi$. Finally, variables $\delta_{\pi(i)jk}$ and $\mu_{\pi(i)jk}$ are (respectively) the amount of energy charged and the battery level when the charging finishes on the segment between breakpoints $k-1$ and $k \in B$ at CS $j \in F$ before the visit to vertex $\pi(i) \in \Pi$. The MILP formulation of the FRVCP follows:

$$\min \quad \sum_{\pi(i)\in\Pi\setminus\{\pi(0)\}} \sum_{j\in F} \sum_{k\in B\setminus\{0\}} \frac{\delta_{\pi(i)jk}}{\rho_{jk}} + \sum_{\pi(i)\in\Pi\setminus\{\pi(0)\}} \sum_{j\in F} \varepsilon_{\pi(i)j}\big(t_{\pi(i-1)j} + t_{j\pi(i)} - t_{\pi(i-1)\pi(i)}\big) \qquad (1)$$

9

Subject to

$$\phi_{\pi(1)} = Q - \sum_{j \in F} \varepsilon_{\pi(1)j} e_{\pi(0)j} - e_{\pi(0)\pi(1)} \left(1 - \sum_{j \in F} \varepsilon_{\pi(1)j} \right) \tag{2}$$

$$\phi_{\pi(i)} = \phi_{\pi(i-1)} + \sum_{j \in F} \sum_{k \in B \setminus \{0\}} \delta_{\pi(i-1)jk} - \sum_{j \in F} \varepsilon_{\pi(i-1)j} e_{j\pi(i-1)} -$$

$$\sum_{j \in F} \varepsilon_{\pi(i)j} e_{\pi(i-1)j} - e_{\pi(i-1)\pi(i)} \left(1 - \sum_{j \in F} \varepsilon_{\pi(i)j} \right) \qquad \forall \pi(i) \in \Pi \setminus \{\pi(0), \pi(1), \pi(n_r)\} \tag{3}$$

$$\phi_{\pi(n_r)} = \phi_{\pi(n_r-1)} + \sum_{j \in F} \sum_{k \in B \setminus \{0\}} \delta_{\pi(n_r-1)jk} +$$

$$\sum_{j \in F} \sum_{k \in B \setminus \{0\}} \delta_{\pi(n_r)jk} - \sum_{j \in F} \varepsilon_{\pi(n_r-1)j} e_{j\pi(n_r-1)} -$$

$$\sum_{j \in F} \varepsilon_{\pi(n_r)j} \left(e_{\pi(n_r-1)j} + e_{j\pi(n_r)} \right) - e_{\pi(n_r-1)\pi(n_r)} \left(1 - \sum_{j \in F} \varepsilon_{\pi(n_r)j} \right) \tag{4}$$

$$\phi_{\pi(n_r-1)} + \sum_{j \in F} \sum_{k \in B \setminus \{0\}} \delta_{\pi(n_r-1)jk} - \sum_{j \in F} e_{j\pi(n_r-1)} \varepsilon_{\pi(n_r-1)j} -$$

$$\sum_{j \in F} e_{\pi(n_r-1)j} \varepsilon_{\pi(n_r)j} \right) \geq 0 \tag{5}$$

$$\mu_{\pi(i)j1} = \phi_{\pi(i)} + \delta_{\pi(i)j1} \qquad \forall \pi(i) \in \Pi \setminus \{\pi(0)\}, \forall j \in F \tag{6}$$

$$\mu_{\pi(n_r)j1} = \phi_{\pi(n_r-1)} + \sum_{l \in F} \sum_{k \in B \setminus \{0\}} \delta_{\pi(n_r-1)lk} -$$

$$\sum_{l \in F} e_{l\pi(n_r-1)} \varepsilon_{\pi(n_r-1)l} - \varepsilon_{\pi(n_r)j} e_{\pi(n_r-1)j} + \delta_{\pi(n_r)j1} \qquad \forall \pi(i) \in \Pi \setminus \{\pi(0)\}, \forall j \in F \tag{7}$$

$$\mu_{\pi(i)jk} = \mu_{\pi(i)j,k-1} + \delta_{\pi(i)jk} \qquad \forall \pi(i) \in \Pi \setminus \{\pi(0)\}, \forall j \in F, \forall k \in B \setminus \{0,1\} \tag{8}$$

$$\mu_{\pi(i)jk} \geq a_{jk-1} \theta_{\pi(i)jk} \qquad \forall \pi(i) \in \Pi \setminus \{\pi(0)\}, \forall j \in F, \forall k \in B \setminus \{0,1\} \tag{9}$$

$$\mu_{\pi(i)jk} \leq a_{jk} \theta_{\pi(i)jk} + (1 - \theta_{\pi(i)jk}) Q \qquad \forall \pi(i) \in \Pi \setminus \{\pi(0)\}, \forall j \in F, \forall k \in B \setminus \{0\} \tag{10}$$

$$\sum_{j \in F} \varepsilon_{\pi(i)j} \leq 1, \qquad \forall \pi(i) \in \Pi \setminus \{\pi(0)\} \tag{11}$$

$$\theta_{\pi(i)jk} \leq \varepsilon_{\pi(i)j} \qquad \forall \pi(i) \in \Pi \setminus \{\pi(0)\}, \forall j \in F, \forall k \in B \setminus \{0\} \tag{12}$$

$$\delta_{\pi(i)jk} \leq \theta_{\pi(i)jk} Q \qquad \forall \pi(i) \in \Pi \setminus \{\pi(0)\}, \forall j \in F, \forall k \in B \setminus \{0\} \tag{13}$$

$$\bar{t} + \sum_{\pi(i) \in \Pi \setminus \{\pi(0)\}} \sum_{j \in F} \sum_{k \in B \setminus \{0\}} \frac{\delta_{\pi(i)jk}}{\rho_{jk}} +$$

$$\sum_{\pi(i) \in \Pi} \sum_{j \in F} \varepsilon_{\pi(i)j} (t_{\pi(i-1)j} + t_{j\pi(i)} - t_{\pi(i-1)\pi(i)}) \leq T_{max} \tag{14}$$

$$\phi_{\pi(i)} \geq 0, \qquad \forall \pi_i \in \Pi \setminus \{\pi(0)\} \tag{15}$$

$$\varepsilon_{\pi(i)j} \in \{0,1\}, \qquad \forall \pi(i) \in \Pi \setminus \{\pi(0)\}, \forall j \in F \tag{16}$$

$$\theta_{\pi(i)jk} \in \{0,1\} \qquad \forall \pi(i) \in \Pi \setminus \{\pi(0)\}, \forall j \in F, \forall k \in B \setminus \{0\} \tag{17}$$

$$\delta_{\pi(i)jk} \geq 0 \qquad \forall \pi(i) \in \Pi \setminus \{\pi(0)\}, \forall j \in F, \forall k \in B \setminus \{0\} \tag{18}$$

$$\mu_{\pi(i)jk} \geq 0 \qquad \forall \pi(i) \in \Pi \setminus \{\pi(0)\}, \forall j \in F, \forall k \in B \setminus \{0\} \tag{19}$$

The objective function (1) seeks to minimize the total route time (including charging and detour times). Constraints (2-5) define the battery level when the EV arrives at vertex $\pi(i) \in \Pi$ if $\varepsilon_{\pi(i)j} = 0$; or to CS $j \in F$ before visiting vertex $\pi(i) \in \Pi$, if $\varepsilon_{\pi(i)j} = 1$. Constraints (6-8) define the battery level when the EV finishes charging at CS $j \in F$ in the segment between breakpoints $k-1$ and $k \in B$ before visiting vertex $\pi(i) \in \Pi$. Constraints (9-10) ensure that if the EV charges on a given segment, the battery level lays between the values of its corresponding break points ($a_{j,k-1}$ and a_{jk}). Constraints (11) state that only one CS is visited between any two vertices of the fixed route. Constraints (12) ensure that the EV only uses segments of visited CSs. Likewise, constraints (13) ensure that the EV charges only at selected segments of visited CSs. Constraint (14) represents the duration constraint of the route. Finally, constraints (15-19) define the domain of the decision variables.

4.2. Solving the FRVCP

To solve the FRVCP, we embedded into our method two different solution approaches. The first consists in solving the MILP introduced in the previous subsection using a commercial solver. The second consist in solving the problem using a greedy heuristic adapted from the literature. The remainder of this subsection describes these approaches.

4.2.1. Approach 1: commercial solver

Because of its verbosity, at first glance the model introduced in Section 4.1 may seem too complex to be efficiently solved using out-of-the-box software. Nonetheless, since in practice the number customers per route and the number of available CSs tend to be low, the resulting MILP formulations are within the scope of commercial solvers. For instance, on an problem with 8 CSs, the MILP formulation for a fixed route serving 10 customers has: 539 continuous variables, 352 integer variables, and 1,263 constraints[2]. We optimally solved that model using Gurobi Optimizer (version 5.6.0) in 0.06s. Based on this observation we decided to embed into our ILS+HC a component that relies on a commercial solver to tackle the FRVCP.

To further reduce the size of the MILP formulation and consequently improve solver's performance, we propose four preprocessing strategies that eliminate infeasible CSs insertions. Our strategies rely on the two following premises: (i) the energy consumption and the travel time between vertices satisfy the triangular inequality; and (ii) since the piecewise-linear charging function is concave (i.e., $\rho_{j,k-1} \geq \rho_{jk}$), the first segment has the fastest charging rate.

We propose two types of strategies. The first three strategies filter CS insertions that are infeasible independently of how the customers are packed and sequenced in the routes. These strategies are applied only once before running the ILS+HC. On the other hand, the fourth strategy filters CS insertions that are infeasible for a particular fixed route.

---

[2]We randomly picked the route from the best solution found to a randomly picked instance

Strategy 1 : This strategy estimates the minimum time τ needed to visit CS $j \in F$ between two vertices i and $h \in I \cup \{0\}$. This time is defined as the sum of a lower bound on the travel time (u) and a lower bound on the charging time (v) of any route serving customers i and h. Note that in any route serving customer i, t_{0i} is a lower bound on the route's duration from the start up to customer i. Similarly, note that in any route servicing customer h, t_{h0} is a lower bound on the time needed to complete a route from vertex h. Based on these two observations we can compute the minimum duration of a route visiting CS j between vertices i and h as $u = t_{0i} + t_{ij} + t_{jh} + t_{h0} + p_i + p_h$. To compute the minimum charging time v, we need to compute the minimum amount of energy (ec) that an EV coming from vertex i and traveling to vertex h must charge at CS j. This amount is the charge needed to recover the energy consumed to make the detour to j, that is, $ec = e_{ij} + e_{jh} - e_{ih}$. Because the battery level when the EV arrives at i in any eVRP-NL solution is unknown a priori, we consider that the battery is charged at j using the fastest charging rate (ρ_{0j}). Then $v = \frac{ec}{\rho_{0j}}$. It is clear that if $\tau = u + v > T_{max}$ any route visiting CS j between customers i and h is infeasible. We therefore forbid this insertion in our MILP.

Strategy 2 : This strategy computes a lower bound on the remaining energy that an EV must have at arrival to customer i to be able to visit CS j right after. Note that in terms of energy remaining, the best way to reach vertex i is to visit it right after fully charging at CS $c(i) = \arg\min_{l \in F \cup \{0\}} e_{li}$. If $Q - e_{c(i)i} < e_{ij}$ any route visiting j after i is energy-infeasible and we can safely forbid this insertion in our MILP.

Strategy 3 : Note that $o = Q - e_{ji}$ is a lower bound on the energy remaining when an EV arrives at customer i right after charging at CS j. Note also that o must be enough to at least close the route (reach the depot) or reach the closest CS in terms of energy consumption. If $o < e_{ic(i)}$, where $c(i) = \arg\min_{l \in F \cup \{0\}} e_{il}$, any route visiting j before i is energy-infeasible and we can safely forbid this insertion.

Strategy 4 : This strategy estimates a lower bound on the new duration of a given fixed route if CS $j \in F$ is inserted between vertices $\pi(i)$ and $\pi(i+1) \in \Pi$, $i \neq n_r$. This bound, $\overline{t'}$, is defined as the sum of the new travel time (u) and a lower bound on the charging time (v). It is easy to see that $u = \overline{t} + t_{\pi(i)j} + t_{j\pi(i+1)} - t_{\pi(i)\pi(i+1)}$. Similarly to Strategy 1, to estimate v, we consider that the battery is charged at j using the fastest charging rate. Therefore $v = \frac{ec}{\rho_{0j}}$, where $ec = e_{\pi(i)j} + e_{j\pi(i+1)} - e_{\pi(i)\pi(i+1)}$ is the charge needed to recover the energy consumed in the detour to j. If $\overline{t'} = (u + v) > T_{max}$, inserting j between vertices $\pi(i)$ and $\pi(i+1)$ leads to an infeasible route, so we can safely forbid this insertion.

Applying our preprocessing strategies to the MILP formulation for the 10-customer route of the example above, the model reduces to: 71 continuous variables, 40 integer variables, and 165 constraints. We solved the model in Gurobi in 0.02s.

4.2.2. Approach 2: greedy heuristic

Existing metaheuristics for eVRPs use different approaches to make charging decisions. One popular approach is the *recharge relocation operator* proposed by Felipe et al. (2014) for the green vehicle routing problem with multiple technologies and partial recharges (GVRP-MTPR). This approach considers the insertion of only one CS per route. Starting from an energy-feasible fixed-route the procedure first deletes the current CS. Then, it tries to improve the charging decisions by inserting each CS into each arc of the fixed-route. To decide how much energy to charge at the inserted CS, the algorithm applies a simple rule: charge the minimum amount of energy needed to reach the depot (i.e., to complete the route). We propose here a heuristic to solve the FRVCP based on this approach.

Our heuristic works in two phases: *location of CSs* and *charge setting*. In the first phase, the heuristic iteratively inserts CSs into the arcs of the fixed-route Π in order to ensure the feasibility in terms of energy. In the second phase, the heuristic improves the charging decisions by adjusting the energy charged at each visited CS. Algorithm 1 describes the structure of our heuristic. It uses four important procedures `trackBattery`$(\cdot)$, `sumNegative`$(\cdot)$, `totalTime`$(\cdot)$, and `copyAndInsert`$(\cdot)$. Procedure `trackBattery`$(\cdot)$ computes the battery level Y_i at each vertex $i \in \Pi$, assuming that the EV fully charges its battery at each visited CS. Note that Y_i may take negative values. Procedure `sumNegative`$(\cdot)$ computes the sum of the battery levels with negative values (i.e., $s = \sum_{i \in \Pi} min\{0, Y_i\}$). Procedure `totalTime`$(\cdot)$ computes the total time t of the route (supposing a full charging policy). Finally, procedure `copyAndInsert`$(\cdot)$ takes as input a fixed route, a CS, and a position in the route; and returns a copy of the fixed route with the CS inserted at the given position.

The heuristic starts by the location phase (line 2-27). After computing s for the current fixed-route Π, the heuristic enters the outer loop (line 7-27). In each pass through the inner loop (line 8-25), the heuristic: i) evaluates the insertion of a CS into each arc of Π assuming that the EV fully charges its battery, and ii) selects the insertion that maximizes s (lines 14-18). If $s = 0$ (i.e., the route is energy-feasible), the heuristic selects the insertion that minimizes t (line 19-23). Then, the heuristic performs the selected insertion (line 26). If the route Π is still energy-infeasible (i.e., $s < 0$), the heuristic starts again at line 8 and tries to insert additional CSs until feasibility in terms of energy is reached.

In the charge setting phase (line 28), the heuristic invokes procedure `ruleMinEnergy`(Π) to set the energy charged at each CS following the Felipe et al. (2014) rule. Finally, the heuristic evaluates if the route satisfies the maximum-duration constraint (29-33). The heuristic returns a boolean variable indicating whether or not the fixed-route is feasible (f), and the route Π with the newly inserted CSs.

Algorithm 1 Greedy heuristic

 1: **function** GREEDYHEURISTIC(Π^0,F)
 2:     $\Pi \longleftarrow \Pi^0$
 3:     $Y \longleftarrow \texttt{trackBattery}(\Pi)$
 4:     $s \longleftarrow \texttt{sumNegative}(Y)$
 5:     $t \longleftarrow \infty$
 6:     $f \longleftarrow \text{false}$
 7:     **while** $s < 0$ **do**
 8:         **for** $j = 1$ to $|F|$ **do**
 9:             **for** $i = 0$ to $n_r - 1$ **do**
10:                 $\Pi' \longleftarrow \texttt{copyAndInsert}(\Pi, F_j, i)$
11:                 $Y' \longleftarrow \texttt{trackBattery}(\Pi')$
12:                 $s' \longleftarrow \texttt{sumNegative}(Y')$
13:                 $t' \longleftarrow \texttt{totalTime}(\Pi')$
14:                 **if** $s' > s$ **then**
15:                     $s \longleftarrow s'$
16:                     $u \longleftarrow j$
17:                     $v \longleftarrow i$
18:                 **end if**
19:                 **if** $s' = 0$ and $t' < t$ **then**
20:                     $t \longleftarrow t'$
21:                     $u \longleftarrow j$
22:                     $v \longleftarrow i$
23:                 **end if**
24:             **end for**
25:         **end for**
26:         $\Pi \longleftarrow \texttt{copyAndInsert}(\Pi, F_u, i)$
27:     **end while**
28:     $\langle t, \Pi \rangle \longleftarrow \texttt{RuleMinEnergy}(\Pi)$
29:     **if** $t \leq T_{max}$ **then**
30:         $f \longleftarrow \text{true}$
31:     **else**
32:         $\Pi \longleftarrow \Pi^0$
33:     **end if**
34:     **return** f, Π
35: **end function**

---

5. Computational experiments

In this section, we present three computational studies. The first study compares the quality of the solutions obtained by two versions of our metaheuristic. The second study evaluates the CPU time of our metaheuristic, and assesses the impact of the preprocessing

strategies. Finally, the third study analyses the charging decisions of the best solutions found.

5.1. Test instances for the eVRP-NL

To test our approach, we generated a new 120-instance testbed built using real data of EV configuration and battery charging functions. In order to ensure feasibility, we opted to generate our instances instead of adapting a existing dataset from the literature. To build the instances we first generated 30 sets of customer locations with {10, 20, 40, 80, 160, 320} customers. For each instance size, we generated 5 sets of customers location. We located the customers in a geographic space of 120 x 120 km using either a random uniform distribution, a random clustered distribution, or a mixture of both. For each of the 30 sets of locations we chose the customer location strategy using a uniform probability distribution. Our main motivation to choose a 120 x 120 geographic area was to build instances representing a semi-urban operation. These operations are the best suited applications for eVRPs. Indeed, in city operations routes tend to be sufficiently short to be covered without mid-route charging. On the opposite side, in rural operations routes tend to be long enough to required multiple mid-route charges but access to charging infrastructure is very limited (at least for 2016 standards).

From each of the 30 sets of locations we built 4 instances varying the level of charging infrastructure availability and the strategy used to locate the CSs. We considered two levels of charging infrastructure availability: low and high. To favor feasibility, for each combination of number of customers and infrastructure availability level we handpicked the number CSs as a proportion of the number of customers. We located the CSs either randomly or using a simple p-median heuristic. Our p-median heuristic starts from a set of randomly generated CS locations and iteratively moves those locations trying to minimize the total distance between the CSs and the customers. In our instances, we included three types of CSs: slow, moderate, and fast. For each CS we randomly selected the type using a uniform probability distribution.

The EVs in our instances are Peugeot Ion. This EV has a consumption rate of $0.125\,\mathrm{kWh/km}$, and a battery of $16\,\mathrm{kWh}$. Note that an EV with this characteristics is well suited to service applications such as homecare routing. In reality the exact energy consumption on an arc (e_{ij}) varies with parameters such as the cumulative elevation gain, the external temperature, the speed, and the use of peripherals (e.g., the radio). Nonetheless, for the sake of simplicity we followed the classical approach in the literature and assumed that the energy consumption on an arc is simply the EV's consumption rate multiplied by the arc's distance. To generate the charging functions we fit piece-wise linear functions to the real charging data for a $16\,\mathrm{kWh}$ battery provided by Uhrig et al. (2015). Figure 5 depicts our piece-wise linear approximations. Finally, the maximum route duration for every instance was fixed to 10 hours. Our 120 instances are publicly available at `www.vrp-rep.org` (Mendoza et al. 2014)[3].

---

[3]The instances will be made effectively public after the completion of the reviewing process
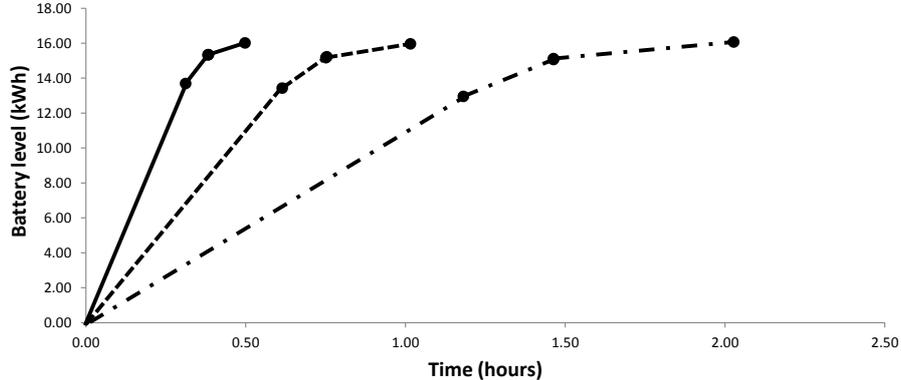
Type of CSs	Slow	Moderate	Fast
Charging power (kWh/h)	11	22	44
Piecewise linear approximation	— · —	------	——

Figure 5: Piecewise linear approximation for different types of CS charging an EV with a battery of 16 kWh.

5.2. Parameter settings & experimental environment

As discussed in Section 4.2 our ILS+HC can be configured to solve the FRVCP using two different approaches, namely, the commercial solver and the greedy heuristic. We tested our algorithm with two different configurations. The first configuration (ILS(S)+HC) uses the commercial optimizer to solve the FRVCP in the GCI neighborhood, while the second configuration (ILS(H)+HC) uses the greedy heuristic. In both configurations, the algorithm solves the FRVCP in the split procedure using the greedy heuristic. This choice was guided by computational performance.

To fine tune the number of iterations of the ILS component (i.e., K), we conducted a short computational study. Our results showed that $K = 80$ provides the best trade-off between solution quality and computational performance. For the sake of brevity we do not discuss the study in this paper.

We implemented our ILS in Java (jre V.1.8.0) and used Gurobi Optimizer (version 5.6.0) to solve the FRVCP and the set partitioning problem in the HC component. We set a time limit of 800 seconds on Gurobi to control the running time of the HC phase. All the experiments were run on a computing cluster with 2.33 GHz Inter Xeon E5410 processors with 16 GB of RAM running under Linux Rocks 6.1.1. The results delivered by the two ILS+HC configurations are compared over 10 runs. Each replication of the experiments was run on a single processor.

5.3. Solution accuracy: optimal vs. heuristic charging decisions

Since the eVRP-NL is a new problem, there are no results or algorithms to benchmark against. To get an idea of the quality of the solutions delivered by our ILS+HC, we ran its two versions, ILS(S)+HC and ILS(H)+HC, on the twenty 10-customer instances and compared their results with optimal solutions found using the MILP for the eVRP-NL presented in

16

the supplementary material. Table 1 summarizes the results comparing the two algorithms under the light of four metrics: the number of optimal solutions found, the average and maximum gap with respect to the optimal solution over the 10 runs, and the average best gap[4]. AppendixA presents detailed results for the 20 instances.

Table 1: Comparison of the two versions of the metaheuristic on small instances with proven optima

Metric	ILS(H)+HC	ILS(S)+HC
Number of optimal solutions	15/20	20/20
Avg. Gap (%)	1.97	0.34
Max. Gap (%)	17.07	1.87
Avg. Best Gap (%)	1.20	0.00

The results suggest that our algorithms are able to deliver high-quality solutions for the eVRP-NL. As shown in the table, ILS(S)+HC matched the 20 optimal solutions while ILS(H)+HC matched 15. The spread in the number of optimal solutions and the values reported for Avg. Best Gap tip the balance towards ILS(S)+HC over ILS(H)+HC in terms accuracy. This result is not surprising since one could expect that making optimal, instead of heuristic, charging decisions would translate into higher quality solutions. A close look at the Avg. and Max. gaps reveals a less foreseeable result: ILS(S)+HC exhibits a significantly more stable behavior than ILS(H)+HC.

To compare the performance of ILS(S)+HC and ILS(H)+HC on more industrial-sized instances we ran both algorithms on the remaining 100 benchmarks. Table 2 summarizes the results. In the comparison we employed the same metrics introduced above, replacing the number of optimal solutions by the number of best known solutions (BKSs) found. As a reference, we included in the table the results delivered by the commercial solver running the MILP for 10h. It is worth mentioning that Gurobi reported integer solutions for only 25 out of the 100 instances. None of these 25 solutions has a certificate of optimality. Detailed results for each instance can be found in AppendixA.

The results in Table 2 confirm the conclusions drawn on our first experiment: optimally solving the FRVCP in the ICG neighborhood leads to a more accurate and stable solution method. According to our data, ILS(S)+HC not only found the 100 BKSs but also reported significantly lower Avg. and Max. gaps (1.51% and 4.44% vs. 7.51% and 28.68%).

5.3.1. The cost of making optimal charging decisions

In Section 5.3 we showed the benefits of making optimal charging decisions when solving the eVRP-NL. This benefits, however, comes at the price of losing computational performance. To estimate this loss, we measured the execution times of three versions of our algorithm on the 120 instances: ILS(S)+HC, ILS(H)+HC, and ILS(S')+HC. The latter is a version of ILS(S)+HC running without our preprocessing strategies (see §4.2.1). Table 3

---

[4]The best gap is the gap between the best solution found over 10 runs and the optimal solution

Table 2: Comparison of the two versions of the metaheuristic on large instances

Metric	Gurobi	ILS(H)+HC	ILS(S)+HC
Number of solutions	25/100	100/100	100/100
Number of BKSs	7/100	7/100	100/100
Avg. Gap (%)	41.36	7.51	1.51
Max. Gap (%)	NA	28.68	4.44
Avg. Best Gap (%)	NA	5.28	0.00

reports for each instance size, the average execution time (in seconds) of each algorithm. In addition, the last column of the table reports the average speedup between ILS(S′)+HC and ILS(S)+HC (measured as the ratio of their execution times).

Not surprisingly, the results show that ILS(H)+HC is the fastest approach. It is interesting to note that in relative terms, the gap in computational performance between ILS(H)+HC and ILS(S)+HC decreases with the size of the instance. This behavior can be explained by the positive correlation between the instance size and the time needed to solve the set partitioning model in the HC phase. Indeed, the latter heavily depends on the size of the pool Ω which, in turn, is more correlated to the size of the instance than to the strategy used to generate the routes. In other words, on large instances both algorithms spend around the same (considerable) amount of time solving the HC phase. As a consequence, the performance gap in the ILS phase becomes less remarkable.

A second interesting conclusion from this study is that the preprocessing strategies have a remarkable positive impact on the computational performance of the algorithm. As the table shows, on average, the strategies are responsible for a 1.65 speedup on the execution time. The data also suggests that the speedup is independent of the size of the instance. A plausible explanation for this behavior is that for a given instance both ILS(S)+HC and ILS(S')+HC evaluate around the same number of routes during the ILS phase.

Table 3: Average computing time (in seconds) of different variants of the metaheuristic

Instance size	ILS(H)+HC	ILS(S′)+HC	ILS(S)+HC	Speedup
10	0.64	8.54	5.62	1.52
20	1.75	17.47	10.56	1.65
40	8.48	64.16	35.35	1.82
80	39.35	148.76	80.11	1.86
160	289.08	976.84	568.02	1.72
320	2,568.94	5,759.67	4,397.64	1.31
Average	484.71	1,162.57	849.55	1.65
Max	4,766.36	10,335.56	7,636.50	2.53
Min	0.49	3.71	2.36	1.16

ILS(S)+HC and ILS(S′)+HC are the hybrid metaheuristic with and without preprocessing strategies, respectively

18

5.3.2. Characteristics of good eVRP-NL solutions

We analyze in this section the characteristics of the BKSs found in our experiments. We aim to provide the reader with some insight that may be useful when designing new solution methods for the eVRP-NL.

In total, our BKSs are made up of 1,426 routes. Our first analysis concerns the fraction of those routes that exploit mid-route charging. Figure 6 presents the percentage of routes with and without visits to CSs grouped by instance size. The data shows that on average 71.47% of the routes in the BKSs visit at least one CS. This percentage is roughly the same for each instance size. This figure provides two insights. First, mid-route charging is a key element of good eVRP-NL solutions (probably because it gives algorithms flexibility to better pack the customers into the routes). Second, since charging decisions concern most of the routes making up a good solution, they play a critical role in its quality. The latter observation helps explaining the spread on accuracy between ILS(S)+HC and ILS(H)+HC found in the computational studies reported in §5.3.
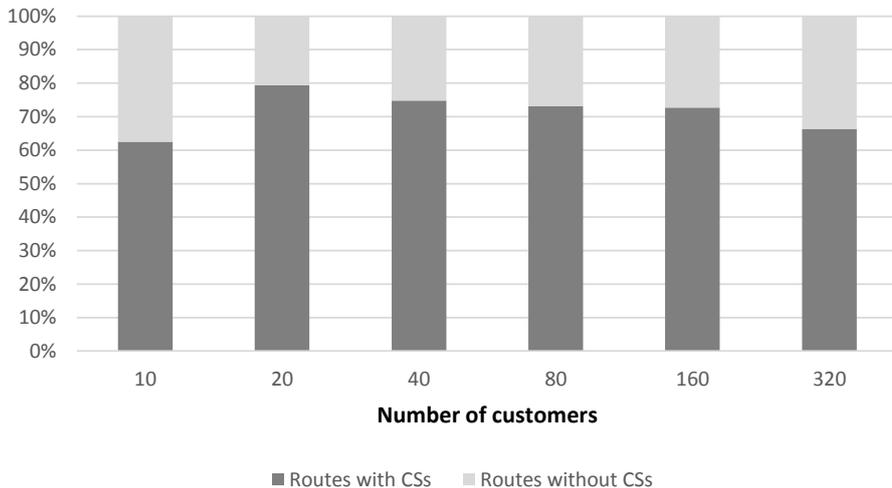
Figure 6: Percentage of the routes with/without visits to CSs by instance size.

The second analysis concerns the number of mid-route charges per route. Figure 7a and 7b present histograms of the number mid-route charges per route and the maximum number of mid-route charges per route on a solution. Figure 7a shows that among the routes performing mid-route charging, 58.58% do it once, 40.00% twice, and 1.43% three times. Although a large portion of the routes perform a single mid-route charge, 85.83% of the solutions contain at least one route performing more than one mid-route charge (Figure 7b). This figures suggest that models and methods for the eVRP-NL can benefit from relaxing the at-the-most-one-visit-to-a-CS-per-route constraint that is sometimes used in the eVRP literature.

The third analysis concerns the energy recovered through mid-route charges. Figure 8 presents the histogram of the average battery level (in % of the total battery capacity)

19
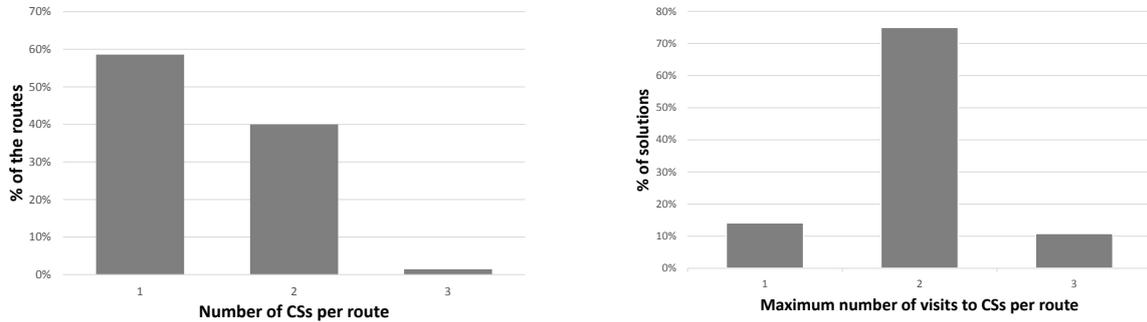
(a) Histogram of number of visits to CS per route.

(b) Histogram of the maximum number of visited CSs in the routes of each solution.

Figure 7: Analysis of the number of visits to CSs

after a mid-route charge. The numbers show that over 90% of the mid-route charges are partial charges (i.e., they do not fully charge the battery). This figure tips the importance of embedding components capable of making partial charging decisions into eVRP-NL solution methods[5]. A second interesting observation from the data displayed in Figure 8 comes from the percentage (around 12%) of mid-route charges that restore the battery above 80% of its capacity. As mentioned in the study reported in the supplementary material, one common assumption in the eVRP literature is that the battery can only be charge on the linear segment of the charging curve (which ends at roughly 80% of the battery capacity). Our data suggest that good eVRP-NL solutions often include routes with mid-route charges that take the battery level up to the non-linear part of the charging function.

---

[5]Note that up to 2016 this was rather the exception than the rule in the eVRP literature
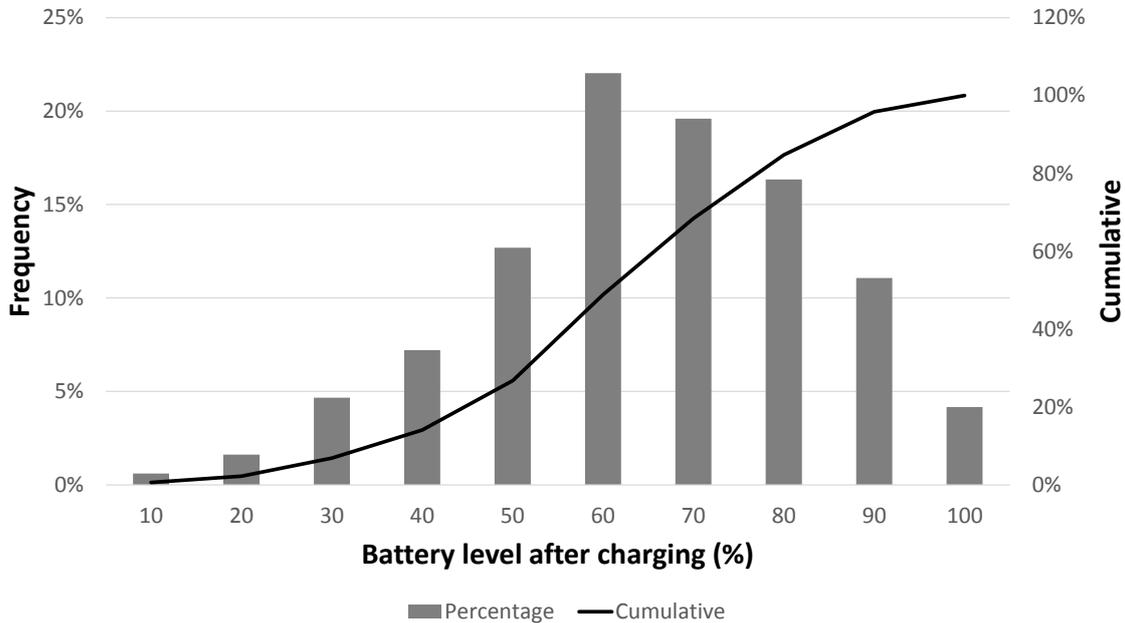
Figure 8: Histogram of the average battery level (in % of the total battery capacity) after a mid-route charge

6. Conclusion and future work

This paper introduces an extension of the electric vehicle routing problem which considers more-realistic assumptions about the battery charging process: the electric vehicle routing problem with nonlinear charging function (eVRP-NL). To solve the problem we propose an iterated local search (ILS) enhanced with heuristic concentration (HC). At the heart of the proposed method lays a neighborhood scheme consisting in solving a new variant of the fixed-route vehicle-charging problem (FRVCP). This problem consists in optimizing the charging decisions (where and how much to charge) of a route serving a fixed sequence of customers. Depending on the configuration, our ILS+HC solves the underlying FRVCP either using a greedy heuristic or a commercial solver. To improve the performance of the solver, we proposed four preprocessing strategies that eliminate infeasible detours to CSs. To assess the performance of our method, we built a set of 120 instances based on real EV and battery charging data. Tested on 20 small 10-customer instances, our method matched the optimal solutions for every instance. Experiments conducted on larger instances proved the value of equipping eVRP-NL algorithms with components capable of making optimal charging decisions. Finally, we analyzed the solutions delivered by our method aiming to provide fellow researchers with some insight into the characteristics of good eVRP-NL solutions. Our analysis concluded that good eVRP-NL solutions tend to use multiple mid-route charges, exploit partial recharges, and employ the non-linear segment of the battery charging function.

Interesting research directions include designing alternative eVRP-NL methods (both

exact and heuristic) to have a better base of comparison for our results. Another interesting perspective is to develop approaches for the FRVCP that offer a different trade off between accuracy and efficiency than those of the two approaches proposed in this paper. In ongoing research, we are extending the problem definition to consider a cost objective function, and time windows.

Acknowledgement

AppendixA. Detailed results of the hybrid metaheuristic

Tables A.4 and A.5 show the results of our two ILS versions (i.e, ILS(S)+HC and MILP(H)+HC) for the small and large eVRP-PNL instances. In Table A.4, we compare our results with the optimal solutions found by Gurobi using the MILP formulation. In Table A.5, we compare our results with the best results obtained with Gurobi. For each instance, we report the problem name[6], and the best solution (BKS) taken from the results of Gurobi, ILS(H)+HC or ILS(S)+HC.

For the results obtained with Gurobi, we report the best solution (Best), and the gap with respect to the BKS (G) [7]. For the results obtained with the ILS(H)+HC and ILS(S)+HC, we report the best solution, the average solution (Avg.), and the average computing time (t in seconds) over ten runs. For the ILS(S)+HC, we also report the average computing time using the preprocessing procedure (t^*). For the two ILS+HC versions, we provide the gap of the average solution and best solution with reference to the BKS. The last rows of the table summarize the average and maximum BKS gap, the number of times each method found the BKS, and the average and maximum running time. Values in bold indicate that a method found the BKS.

---

[6]tc$\boldsymbol{\alpha}$c$\boldsymbol{\beta}$s$\boldsymbol{\mu}$c$\boldsymbol{\epsilon}$#, where $\boldsymbol{\alpha}$ is the type of the location of the customers (i.e., 0:randomize, 1:cluster, 2: mixture of both), $\boldsymbol{\beta}$ is the number of customers, $\boldsymbol{\mu}$ is the number of the CSs, $\boldsymbol{\epsilon}$ is 't' if we use a p-median heuristic to locate the CSs and 'f' otherwise, and # is the number of the instance for each combination of parameters (i.e., # = 0, 1, 2, 3, 4)

[7]$G(\%) = (of - of_{BKS})/of_{BKS} \times 100$

Table A.4: Results of ILS(H)+HC and ILS(S)+HC on the 20 small instances

		Gurobi		ILS(H)+HC					ILS(S)+HC					
Instance	BKS	Best	G(%)	Best	G(%)	Avg.	G(%)	t (s)	Best	G(%)	Avg.	G(%)	t (s)	t *(s)
tc2c10s2cf0	21.77	**21.77**	0.00	22.49	3.31	22.51	3.40	0.61	**21.77**	0.00	21.77	0.00	10.54	8.53
tc0c10s2cf1	19.75	**19.75**	0.00	**19.75**	0.00	20.12	1.87	0.60	**19.75**	0.00	20.12	1.87	4.59	3.86
tc1c10s2cf2	9.03	**9.03**	0.00	**9.03**	0.00	9.04	0.11	0.57	**9.03**	0.00	9.07	0.44	3.71	2.43
tc1c10s2cf3	16.37	**16.37**	0.00	**16.37**	0.00	16.37	0.00	0.83	**16.37**	0.00	16.37	0.00	7.58	5.63
tc1c10s2cf4	16.10	**16.10**	0.00	**16.10**	0.00	16.13	0.19	0.66	**16.10**	0.00	16.10	0.00	6.67	4.79
tc2c10s2ct0	12.45	**12.45**	0.00	**12.45**	0.00	12.53	0.64	0.49	**12.45**	0.00	12.45	0.00	8.36	5.38
tc0c10s2ct1	12.30	**12.30**	0.00	**12.30**	0.00	12.35	0.41	0.62	**12.30**	0.00	12.34	0.33	6.08	3.99
tc1c10s2ct2	10.75	**10.75**	0.00	10.76	0.09	10.77	0.19	0.54	**10.75**	0.00	10.75	0.00	6.51	4.21
tc1c10s2ct3	13.17	**13.17**	0.00	**13.17**	0.00	14.16	7.52	0.84	**13.17**	0.00	13.18	0.08	9.85	7.56
tc1c10s3ct4	13.21	**13.21**	0.00	**13.21**	0.00	13.25	0.30	0.68	**13.21**	0.00	13.21	0.00	11.06	6.01
tc2c10s3cf0	21.77	**21.77**	0.00	22.49	3.31	22.51	3.40	0.61	**21.77**	0.00	21.77	0.00	11.86	8.90
tc0c10s3cf1	19.75	**19.75**	0.00	**19.75**	0.00	20.12	1.87	0.63	**19.75**	0.00	20.12	1.87	6.46	4.41
tc1c10s3cf2	9.03	**9.03**	0.00	9.03	0.00	9.04	0.11	0.56	**9.03**	0.00	9.06	0.33	4.11	2.36
tc1c10s3cf3	16.37	**16.37**	0.00	**16.37**	0.00	16.37	0.00	0.82	**16.37**	0.00	16.37	0.00	9.50	6.06
tc1c10s3cf4	14.90	**14.90**	0.00	**14.90**	0.00	14.94	0.27	0.62	**14.90**	0.00	14.90	0.00	11.27	6.72
tc2c10s3ct0	11.51	**11.51**	0.00	11.54	0.26	11.65	1.22	0.51	**11.51**	0.00	11.54	0.26	11.18	6.81
tc0c10s3ct1	10.80	**10.80**	0.00	**10.80**	0.00	10.81	0.09	0.60	**10.80**	0.00	10.80	0.00	8.91	4.83
tc1c10s3ct2	9.20	**9.20**	0.00	10.76	16.96	10.77	17.07	0.54	**9.20**	0.00	9.34	1.52	9.66	5.33
tc1c10s3ct3	13.02	**13.02**	0.00	**13.02**	0.00	13.12	0.77	0.64	**13.02**	0.00	13.02	0.00	15.72	9.77
tc1c10s2ct4	13.83	**13.83**	0.00	**13.83**	0.00	13.83	0.00	0.77	**13.83**	0.00	13.83	0.00	7.08	4.84
Avg. Gap			0.00		1.20		1.97			0.00		0.34		
Max. Gap			-		16.96		17.07			0.00		1.87		
Best		20		15					20					
Avg. Time								0.64					8.54	5.62
Max. Time								0.84					15.72	9.77

Table A.5: Results of ILS(H)+HC and ILS(S)+HC on the 100 large instances

		Gurobi		ILS(H)+HC					ILS(S)+HC					
Instance	BKS	Best	G(%)	Best	G(%)	Avg.	G(%)	t (s)	Best	G(%)	Avg.	G(%)	t (s)	t *(s)
tc2c20s3cf0	24.68	24.73	0.20	**24.68**	0.00	24.71	0.12	2.14	**24.68**	0.00	24.68	0.00	22.12	13.86
tc1c20s3cf1	17.50	17.55	0.29	17.51	0.06	17.68	1.03	1.39	**17.50**	0.00	17.53	0.17	19.54	12.32
tc0c20s3cf2	27.60	28.54	3.41	27.61	0.04	27.65	0.18	3.14	**27.60**	0.00	27.66	0.22	16.06	11.77
tc1c20s3cf3	16.63	16.81	1.08	**16.63**	0.00	16.79	0.96	1.41	**16.63**	0.00	16.78	0.90	13.15	8.41
tc1c20s3cf4	17.00	**17.00**	0.00	**17.00**	0.00	17.00	0.00	1.20	**17.00**	0.00	17.00	0.00	5.77	3.77
tc2c20s3ct0	25.79	**25.79**	0.00	**25.79**	0.00	25.80	0.04	2.38	**25.79**	0.00	25.79	0.00	23.31	14.66
tc1c20s3ct1	18.95	19.38	2.27	19.55	3.17	19.65	3.69	1.58	**18.95**	0.00	19.38	2.27	23.49	15.25
tc0c20s3ct2	17.08	17.11	0.18	**17.08**	0.00	17.18	0.59	1.73	**17.08**	0.00	17.13	0.29	12.49	8.49
tc1c20s3ct3	12.65	12.68	0.24	12.75	0.79	12.82	1.34	1.76	**12.65**	0.00	12.72	0.55	15.36	8.86
tc1c20s3ct4	16.21	**16.21**	0.00	16.25	0.25	16.31	0.62	1.26	**16.21**	0.00	16.25	0.25	9.74	5.16
tc2c20s4cf0	24.67	25.36	2.80	25.29	2.51	25.35	2.76	1.77	**24.67**	0.00	24.69	0.08	25.90	14.63
tc1c20s4cf1	16.39	16.40	0.06	17.16	4.70	17.47	6.59	1.53	**16.39**	0.00	16.40	0.06	27.19	13.47
tc0c20s4cf2	27.48	-	-	27.60	0.44	27.65	0.62	3.04	**27.48**	0.00	27.61	0.47	18.53	12.81
tc1c20s4cf3	16.56	16.80	1.45	16.80	1.45	16.84	1.69	1.44	**16.56**	0.00	16.80	1.45	14.77	8.69
tc1c20s4cf4	17.00	**17.00**	0.00	**17.00**	0.00	17.00	0.00	1.17	**17.00**	0.00	17.00	0.00	7.61	4.17
tc2c20s4ct0	26.02	-	-	26.49	1.81	26.51	1.88	2.01	**26.02**	0.00	26.02	0.00	25.92	15.25
tc1c20s4ct1	18.25	**18.25**	0.00	19.51	6.90	19.65	7.67	1.58	**18.25**	0.00	18.32	0.38	27.11	16.14
tc0c20s4ct2	16.99	17.21	1.29	17.06	0.41	17.12	0.77	1.62	**16.99**	0.00	17.10	0.65	15.25	9.33
tc1c20s4ct3	14.43	**14.43**	0.00	14.56	0.90	14.58	1.04	1.41	**14.43**	0.00	14.50	0.49	14.30	7.99
tc1c20s4ct4	17.00	**17.00**	0.00	**17.00**	0.00	17.00	0.00	1.49	**17.00**	0.00	17.00	0.00	11.74	6.08
tc0c40s5cf0	32.67	-	-	33.84	3.58	34.53	5.69	6.09	**32.67**	0.00	33.25	1.78	46.66	23.85
tc1c40s5cf1	65.16	-	-	65.32	0.25	66.64	2.27	11.90	**65.16**	0.00	66.03	1.34	65.41	44.01
tc2c40s5cf2	27.54	38.93	41.36	28.22	2.47	28.86	4.79	7.67	**27.54**	0.00	27.67	0.47	48.50	31.64
tc2c40s5cf3	19.74	21.04	6.59	20.44	3.55	20.82	5.47	4.70	**19.74**	0.00	20.18	2.23	30.49	16.85
tc0c40s5ct0	30.77	36.47	18.52	33.06	7.44	34.21	11.18	11.08	**30.77**	0.00	31.49	2.34	49.91	33.33
tc0c40s5ct0	28.72	-	-	29.22	1.74	29.78	3.69	8.55	**28.72**	0.00	29.35	2.19	41.76	24.50
tc1c40s5ct1	52.68	-	-	54.54	3.53	55.05	4.50	12.64	**52.68**	0.00	53.36	1.29	94.40	58.52
tc2c40s5ct2	26.91	-	-	26.99	0.30	27.15	0.89	8.18	**26.91**	0.00	27.02	0.41	38.38	22.85
tc2c40s5ct3	23.54	-	-	23.56	0.08	23.90	1.53	5.77	**23.54**	0.00	23.77	0.98	43.87	26.48
tc0c40s5ct4	28.63	-	-	29.72	3.81	30.84	7.72	10.49	**28.63**	0.00	28.72	0.31	45.55	32.55
tc0c40s8cf0	31.28	-	-	32.73	4.64	33.68	7.67	6.11	**31.28**	0.00	32.02	2.37	72.91	33.59
tc1c40s8cf1	40.75	-	-	45.86	12.54	50.71	24.44	12.11	**40.75**	0.00	42.33	3.88	108.49	69.99
tc2c40s8cf2	27.15	29.19	7.51	28.05	3.31	28.19	3.83	7.87	**27.15**	0.00	27.31	0.59	57.90	28.92
tc2c40s8cf3	19.66	22.01	11.95	19.86	1.02	20.17	2.59	5.41	**19.66**	0.00	20.24	2.95	45.15	19.46
tc0c40s8cf4	29.32	-	-	32.53	10.95	33.69	14.90	9.93	**29.32**	0.00	29.86	1.84	91.10	43.05
tc0c40s8ct0	26.35	30.29	14.95	27.65	4.93	28.32	7.48	6.01	**26.35**	0.00	26.89	2.05	71.70	28.54
tc1c40s8ct1	40.56	-	-	49.35	21.67	49.85	22.90	11.86	**40.56**	0.00	41.19	1.55	124.31	70.50
tc2c40s8ct2	26.33	-	-	26.82	1.86	27.07	2.81	7.12	**26.33**	0.00	26.71	1.44	58.68	25.64
tc2c40s8ct3	22.71	23.51	3.52	23.26	2.42	23.44	3.21	5.16	**22.71**	0.00	23.23	2.29	63.76	25.25
tc0c40s8ct4	29.20	-	-	29.82	2.12	31.68	8.49	10.93	**29.20**	0.00	29.27	0.24	84.36	47.46
tc0c80s8cf0	39.43	-	-	39.78	0.89	40.52	2.76	31.70	**39.43**	0.00	39.86	1.09	104.77	56.41
tc0c80s8cf1	45.23	-	-	46.48	2.76	47.33	4.64	76.55	**45.23**	0.00	45.73	1.11	183.74	121.27
tc1c80s8cf2	30.81	-	-	32.52	5.55	33.30	8.08	31.57	**30.81**	0.00	31.83	3.31	79.36	50.99
tc2c80s8cf3	32.44	-	-	32.53	0.28	32.90	1.42	43.83	**32.44**	0.00	32.60	0.49	95.72	64.05

23

Table A.5 – continued from previous page

Instance	BKS	Gurobi		ILS(H)+HC					ILS(S)+HC					
		Avg	G(%)	Best	G(%)	Avg.	G(%)	t (s)	Best	G(%)	Avg.	G(%)	t (s)	t *(s)
tc2c80s8cf4	49.29	-	-	50.41	2.27	51.06	3.59	45.59	**49.29**	0.00	49.69	0.81	160.43	99.84
tc0c80s8ct0	41.90	-	-	42.18	0.67	42.89	2.36	27.68	**41.90**	0.00	42.76	2.05	99.20	54.35
tc0c80s8ct1	45.27	-	-	46.39	2.47	47.50	4.93	82.12	**45.27**	0.00	45.85	1.28	195.16	129.66
tc1c80s8ct2	31.74	-	-	32.59	2.68	32.90	3.65	37.77	**31.74**	0.00	32.36	1.95	93.21	59.73
tc2c80s8ct3	32.31	-	-	32.74	1.33	33.41	3.40	25.10	**32.31**	0.00	32.55	0.74	111.47	65.15
tc2c80s8ct4	44.83	-	-	49.08	9.48	50.31	12.22	43.42	**44.83**	0.00	46.61	3.97	178.48	111.24
tc0c80s12cf0	34.64	-	-	36.01	3.95	37.25	7.53	29.39	**34.64**	0.00	35.59	2.74	126.00	57.24
tc0c80s12cf1	42.90	-	-	43.81	2.12	45.51	6.08	35.17	**42.90**	0.00	44.07	2.73	157.55	74.58
tc1c80s12cf2	29.54	-	-	32.61	10.39	33.34	12.86	31.52	**29.54**	0.00	30.73	4.03	112.44	61.34
tc2c80s12cf3	31.97	-	-	34.10	6.66	35.13	9.88	25.63	**31.97**	0.00	32.70	2.28	159.17	75.64
tc2c80s12cf4	43.89	-	-	47.95	9.25	48.57	10.66	50.96	**43.89**	0.00	44.97	2.46	274.06	131.13
tc0c80s12ct0	39.31	-	-	39.97	1.68	40.48	2.98	32.01	**39.31**	0.00	39.83	1.32	159.79	65.54
tc0c80s12ct1	41.94	-	-	42.56	1.48	43.67	4.12	35.06	**41.94**	0.00	43.03	2.60	162.38	73.32
tc1c80s12ct2	29.52	-	-	31.11	5.39	32.33	9.52	29.45	**29.52**	0.00	30.66	3.86	122.60	58.85
tc2c80s12ct3	30.83	-	-	32.09	4.09	32.31	4.80	28.06	**30.83**	0.00	31.59	2.47	123.57	57.57
tc2c80s12ct4	42.40	-	-	47.16	11.23	48.40	14.15	44.51	**42.40**	0.00	42.82	0.99	276.16	134.33
tc1c160s16cf0	79.80	-	-	88.37	10.74	90.49	13.40	298.56	**79.80**	0.00	80.75	1.19	1139.49	765.69
tc2c160s16cf1	60.34	-	-	61.56	2.02	63.57	5.35	181.57	**60.34**	0.00	61.26	1.52	464.11	273.86
tc0c160s16cf2	61.20	-	-	63.85	4.33	65.42	6.90	224.18	**61.20**	0.00	62.99	2.92	600.43	365.10
tc1c160s16cf3	71.76	-	-	73.93	3.02	75.04	4.57	331.06	**71.76**	0.00	72.75	1.38	666.64	461.58
tc0c160s16cf4	82.92	-	-	98.16	18.38	101.13	21.96	536.94	**82.92**	0.00	83.84	1.11	1662.82	1213.20
tc1c160s16ct0	79.04	-	-	83.82	6.05	85.47	8.14	391.41	**79.04**	0.00	79.90	1.09	1012.72	643.27
tc2c160s16ct1	60.27	-	-	61.97	2.82	62.64	3.93	177.27	**60.27**	0.00	60.62	0.58	507.69	287.64
tc0c160s16ct2	60.13	-	-	64.10	6.60	64.50	7.27	204.82	**60.13**	0.00	62.80	4.44	587.52	341.86
tc1c160s16ct3	73.29	-	-	75.29	2.73	76.55	4.45	180.48	**73.29**	0.00	75.11	2.48	483.20	278.67
tc0c160s16ct4	82.37	-	-	95.78	16.28	97.20	18.00	433.62	**82.37**	0.00	83.08	0.86	1413.91	944.60
tc1c160s24cf0	78.60	-	-	85.59	8.89	87.66	11.53	346.79	**78.60**	0.00	79.30	0.89	1343.54	741.12
tc2c160s24cf1	59.82	-	-	61.30	2.47	63.62	6.35	182.55	**59.82**	0.00	61.14	2.21	653.44	304.66
tc0c160s24ct2	59.25	-	-	62.93	6.21	63.31	6.85	206.85	**59.25**	0.00	60.19	1.59	861.85	409.80
tc1c160s24ct3	68.72	-	-	71.78	4.45	74.54	8.47	196.47	**68.72**	0.00	69.98	1.83	756.39	358.35
tc0c160s24cf4	81.44	-	-	95.47	17.23	99.35	21.99	508.19	**81.44**	0.00	82.13	0.85	1984.26	1209.32
tc1c160s24ct0	78.21	-	-	83.38	6.61	84.84	8.48	284.88	**78.21**	0.00	79.35	1.46	1183.70	577.83
tc2c160s24ct1	59.13	-	-	60.84	2.89	62.49	5.68	192.18	**59.13**	0.00	59.72	1.00	748.95	340.40
tc0c160s24cf2	59.27	-	-	62.63	5.67	64.12	8.18	210.13	**59.27**	0.00	60.92	2.78	845.72	403.33
tc1c160s24cf3	68.56	-	-	72.83	6.23	75.18	9.66	240.33	**68.56**	0.00	69.57	1.47	883.61	483.10
tc0c160s24ct4	80.96	-	-	90.55	11.85	93.83	15.90	453.34	**80.96**	0.00	82.11	1.42	1736.76	956.94
tc2c320s24cf0	182.52	-	-	195.23	6.96	210.45	15.30	3762.57	**182.52**	0.00	186.94	2.42	7855.89	6566.41
tc2c320s24cf1	95.51	-	-	97.39	1.97	100.07	4.77	1003.08	**95.51**	0.00	96.42	0.95	1927.61	1456.16
tc1c320s24cf2	152.23	-	-	177.71	16.74	185.68	21.97	3162.07	**152.23**	0.00	153.99	1.16	8370.48	7105.63
tc1c320s24cf3	117.48	-	-	124.23	5.75	126.08	7.32	2089.09	**117.48**	0.00	118.36	0.75	3737.73	3065.82
tc2c320s24cf4	122.88	-	-	134.30	9.29	136.17	10.82	2177.20	**122.88**	0.00	124.68	1.46	4961.50	3681.14
tc2c320s24ct0	181.50	-	-	208.32	14.78	212.18	16.90	4434.40	**181.50**	0.00	186.23	2.61	8606.62	7204.02
tc2c320s24ct1	94.73	-	-	96.69	2.07	99.71	5.26	942.21	**94.73**	0.00	96.49	1.86	1737.70	1259.26
tc1c320s24ct2	148.77	-	-	173.82	16.84	182.34	22.57	3617.64	**148.77**	0.00	154.13	3.60	8231.61	6853.35
tc1c320s24ct3	116.64	-	-	122.75	5.24	125.71	7.78	1984.42	**116.64**	0.00	119.17	2.17	3783.98	3273.79
tc2c320s24ct4	122.02	-	-	131.87	8.07	133.68	9.56	3074.58	**122.02**	0.00	123.85	1.50	5447.73	4273.94
tc2c320s38cf0	177.01	-	-	202.48	14.39	207.83	17.41	4007.13	**177.01**	0.00	182.31	2.99	9150.09	6733.82
tc2c320s38cf1	94.29	-	-	97.55	3.46	99.54	5.57	1082.91	**94.29**	0.00	95.07	0.83	2443.29	1601.78
tc1c320s38cf2	141.68	-	-	173.71	22.61	181.84	28.35	3208.78	**141.68**	0.00	147.08	3.81	9490.84	7235.62
tc1c320s38cf3	116.33	-	-	122.49	5.30	125.30	7.71	2024.26	**116.33**	0.00	117.74	1.21	4600.98	3113.71
tc2c320s38cf4	122.32	-	-	128.72	5.23	131.01	7.10	1814.78	**122.32**	0.00	123.47	0.94	4138.21	2660.68
tc2c320s38ct0	191.09	-	-	205.08	7.32	208.44	9.08	4766.36	**191.09**	0.00	192.15	0.55	10335.56	7636.50
tc2c320s38ct1	94.53	-	-	97.44	3.08	98.62	4.33	938.85	**94.53**	0.00	95.29	0.80	2284.16	1408.88
tc1c320s38ct2	141.14	-	-	172.99	22.57	181.62	28.68	3660.78	**141.14**	0.00	145.09	2.80	9264.46	6974.34
tc1c320s38ct3	116.07	-	-	122.91	5.89	126.17	8.70	1993.12	**116.07**	0.00	117.71	1.41	4559.66	3062.95
tc2c320s38ct4	121.66	-	-	127.40	4.72	130.35	7.14	1634.65	**121.66**	0.00	123.15	1.22	4265.37	2784.91
Avg. Gap		4.71		5.28		7.51			0.00		1.51			
Max. Gap		41.36		22.61		28.68			0.00		4.44			
Found solution		25		100					100					
Best		7		7			3		100					
Avg. Time								581.52					1393.38	1018.33
Max. Time								4766.36					10335.56	7636.50

References

Bansal, P. (2015), 'Charging of electric vehicles: Technology and policy implications', *Journal of Science Policy & Governance* **6**(1).

Becker, T. A., Sidhu, I. & Tenderich, B. (2009), Electric vehicles in the United States: a new model with forecasts to 2030, Technical report.

Bruglieri, M., Colorni, A. & Luè, A. (2014), 'The vehicle relocation problem for the one-way electric vehicle sharing: An application to the Milan case', *Procedia - Social and Behavioral Sciences* **111**, 18 – 27.

Bruglieri, M., Pezzella, F., Pisacane, O. & Suraci, S. (2015), 'A variable neighborhood search branching for the electric vehicle routing problem with time windows', *Electronic Notes in Discrete Mathematics* **47**, 221–228.

Conrad, R. G. & Figliozzi, M. A. (2011), The recharging vehicle routing problem, *in* T. Doolen & E. V. Aken, eds, 'Proceedings of the 2011 Industrial Engineering Research Conference', Reno, NV, USA.

Desaulniers, G., Errico, F., Irnich, S. & Schneider, M. (2014), Exact algorithms for electric vehicle-routing problems with time windows, Technical report, GERAD, G-2014-110.

Electrification-Coalition (2013), 'State of the plug-in electric vehicle market', `http://www.electrificationcoalition.org/sites/default/files/EC_State_of_PEV_Market_Final_1.pdf`. Last accessed 01/01/2016.

Erdoğan, S. & Miller-Hooks, E. (2012), 'A green vehicle routing problem', *Transportation Research Part E: Logistics and Transportation Review* **48**(1), 100–114.

Felipe, A., Ortuño, M. T., Righini, G. & Tirado, G. (2014), 'A heuristic approach for the green vehicle routing problem with multiple technologies and partial recharges', *Transportation Research Part E: Logistics and Transportation Review* **71**, 111 – 128.

Goeke, D. & Schneider, M. (2015), 'Routing a mixed fleet of electric and conventional vehicles', *European Journal of Operational Research* **245**(1), 81 – 99.

Heineken (2013), 'Europe's largest electric truck will drive down emissions', `http://sustainabilityreport.heineken.com/Reducing-CO2-emissions/Case-studies/Europes-largest-electric-truck-will-drive-down-emissions/index.htm`. Last accessed 13/04/2016.

Hiermann, G., Puchinger, J., Ropke, S. & Hartl, R. F. (2016), 'The electric fleet size and mix vehicle routing problem with time windows and recharging stations', *European Journal of Operational Research* **252**(3), 995 –1018.

Hõimoja, H., Rufer, A., Dziechciaruk, G. & Vezzini, A. (2012), An ultrafast ev charging station demonstrator, *in* 'Power Electronics, Electrical Drives, Automation and Motion (SPEEDAM), 2012 International Symposium on', IEEE, pp. 1390–1395.

Keskin, M. & Çatay, B. (2016), 'Partial recharge strategies for the electric vehicle routing problem with time windows', *Transportation Research Part C: Emerging Technologies* **65**, 111 – 127.

Kleindorfer, P. R., Neboian, A., Roset, A. & Spinler, S. (2012), 'Fleet renewal with electric vehicles at La Poste', *Interfaces* **42**(5), 465–477.

Liao, C.-S., Lu, S.-H. & Shen, Z.-J. M. (2016), 'The electric vehicle touring problem', *Transportation Research Part B: Methodological* **86**, 163 – 180.

Loaiza (2014), 'Convenio sura- celsia, por el bien del medio ambiente', `http://www.sura.com/blogs/autos/convenio-sura-celsia-por-el-medio-ambiente.aspx`. Last accessed 13/04/2016.

Lourenço, H. R., Martin, O. C. & Stützle, T. (2010), Iterated local search: Framework and applications, *in* 'Handbook of Metaheuristics', Springer, pp. 363–397.

Mendoza, J. E., Guéret, C., Hoskins, M., Lobit, H., Pillac, V., Vidal, T. & Vigo, D. (2014), VRP-REP: a vehicle routing community repository, *in* 'Third meeting of the EURO Working Group on Vehicle Routing and Logistics Optimization (VeRoLog). Oslo (Norway)'.

Mladenović, N. & Hansen, P. (1997), 'Variable neighborhood search', *Computers & Operations Research* **24**(11), 1097–1100.

Montoya, A., Guéret, C., Mendoza, J. E. & Villegas, J. G. (2015), 'A multi-space sampling heuristic for the green vehicle routing problem', *Transportation Research Part C: Emerging Technologies* p. DOI:10.1016/j.trc.2015.09.009.

Nesterova, N., Quak, H., Balm, S., Roche-Cerasi, I. & Tretvik, T. (2015), Project frevue deliverable d1. 3: State of the art of the electric freight vehicles implementation in city logistics, Technical Report 5, TNO and SINTEF. European Commission Seventh framework programme.

Pelletier, S., Jabali, O. & Laporte, G. (2016), '50th anniversary invited article—goods distribution with electric vehicles: Review and research perspectives', *Transportation Science* **50**(1), 3–22.

Pelletier, S., Jabali, O., Laporte, G. & Veneroni, M. (2015), Goods distribution with electric vehicles:

Battery degradation and behaviour modeling, Technical report, CIRRELT-2015-43.

Post & Parcel (2014), 'CTT group invests 5M of euros in green fleet', `http://postandparcel.info/60290/uncategorized/ctt-group-invests-e5m-in-green-fleet/`. Last accessed 13/04/2016.

Prins, C. (2004), 'A simple and effective evolutionary algorithm for the vehicle routing problem', *Computers & Operations Research* **31**(12), 1985 – 2002.

Ramirez, M. (2015), 'Bimbo inaugura el segundo centro de ventas ecologíco en México', `http://www.milenio.com/negocios/Centro_de_Ventas_Ecologico-bimbo-Centro_de_Ventas_Ecologico_bimbo_0_633536930.html`. Last accessed 13/04/2016.

Rosenkrantz, D., Stearns, R. & Lewis, P. (1974), Approximate algorithms for the traveling salesperson problem, *in* 'Switching and Automata Theory, 1974., IEEE Conference Record of 15th Annual Symposium on', pp. 33–42.

Rosing, K. & ReVelle, C. (1997), 'Heuristic concentration: Two stage solution construction', *European Journal of Operational Research* **97**(1), 75 – 86.

Sassi, O., Cherif-Khettaf, W. & Oulamara, A. (2015), Iterated tabu search for the mix fleet vehicle routing problem with heterogenous electric vehicles, *in* H. A. Le Thi, T. Pham Dinh & N. T. Nguyen, eds, 'Modelling, Computation and Optimization in Information Systems and Management Sciences', Vol. 359 of *Advances in Intelligent Systems and Computing*, Springer International Publishing, pp. 57–68.

Schiffer, M. & Walther, G. (2015), The electric location routing problem with time windows and partial recharging, Technical report, RWTH Aachen University.

Schneider, M., Stenger, A. & Goeke, D. (2014), 'The electric vehicle-routing problem with time windows and recharging stations', *Transportation Science* **48**(4), 500–520.

Schneider, M., Stenger, A. & Hof, J. (2015), 'An adaptive VNS algorithm for vehicle routing problems with intermediate stops', *OR Spectrum* **37**(2), 353–387.

Suzuki, Y. (2014), 'A variable-reduction technique for the fixed-route vehicle-refueling problem', *Computers & Industrial Engineering* **67**, 204–215.

Sweda, T. M., Dolinskaya, I. S. & Klabjan, D. (2016), 'Optimal recharging policies for electric vehicles', *Transportation Science* p. DOI: 10.1287/trsc.2015.0638.

Szeto, W. & Cheng, Y. (2016), Artificial bee colony approach to solving the electric vehicle routing problem, *in* 'Annual Meeting of the Transportation Research Board, TRB 2016'.

TU Delft, HAW Hamburg, L. Z. F. (2013), 'Comparative analysis of european examples of schemes for freight electric vehicles - compilation report. e-mobility nsr', `http://e-mobility-nsr.eu/fileadmin/user_upload/downloads/info-pool/E-Mobility_-_Final_report_7.3.pdf`. Last accessed 01/01/2016.

Uhrig, M., Weiß, L., Suriyah, M. & Leibfried, T. (2015), E-mobility in car parks–guidelines for charging infrastructure expansion planning and operation based on stochastic simulations, *in* 'the 28th International Electric Vehicle Symposium and Exhibition, KINTEX, Korea'.

UPS (2008), 'UPS hybrid electric vehicle fleet.', `http://www.pressroom.ups.com/HEV`. Last accessed 05/14/2014.

Zündorf, T. (2014), Electric vehicle routing with realistic recharging models, Master's thesis, Karlsruhe Institute of Technology, Karlsruhe, Germany.

A comparative study of charging assumptions in electric vehicle routing problems [1]

Alejandro Montoya[a,b], Christelle Guéret[a], Jorge E. Mendoza[c], Juan G. Villegas[d,*]

[a]*Université d'Angers, LARIS (EA 7315), 62 avenue Notre Dame du Lac, 49000 Angers, France*
[b]*Departamento de Ingeniería de Producción, Universidad EAFIT, Carrera 49 No. 7 Sur - 50, Medellín, Colombia*
[c]*Université François-Rabelais de Tours, CNRS, LI (EA 6300), OC (ERL CNRS 6305), 64 avenue Jean Portalis, 37200 Tours, France*
[d]*Departamento de Ingeniería Industrial, Facultad de Ingeniería, Universidad de Antioquia, Calle 70 No. 52-21, Medellín, Colombia*

1. Introduction

The objective of this supplementary material is to compare the assumptions to model the battery charging process that are most commonly found in the eVRP literature. We first present the approximations used for the charging function in transportation planning problems with electric vehicles (EVs). Then, we present a mixed-integer linear programming (MILP) formulation for the electric vehicle routing problem with nonlinear charging function (eVRP-NL) that. With a few minor modifications, the model can be adapted to work with other charging policies and charging function approximations used in the extant eVRP literature. We use the MILP formulation and a commercial solver to evaluate the impact of including the nonlinear charging functions and partial charging in eVRPs. Our results suggest that disallowing partial charging and neglecting the nonlinear nature of the charging functions leads to solutions that may be infeasible or overly expensive.

2. Modeling battery charging functions

The charging function of a battery models the relationship between charging time and charging level. In general, the charging functions are nonlinear, because the terminal voltage and current change during the charging process. This process is divided into two phases. In the first phase, the charging current is held constant, and thus the state of charge (SOC)

---

increases linearly with time until the battery's terminal voltage increases to a specific maximum value (see Figure 1). In the second phase, the current decreases exponentially and the terminal voltage is held constant to avoid battery damages. The SOC increases then concavely with the time (Pelletier et al. 2015).
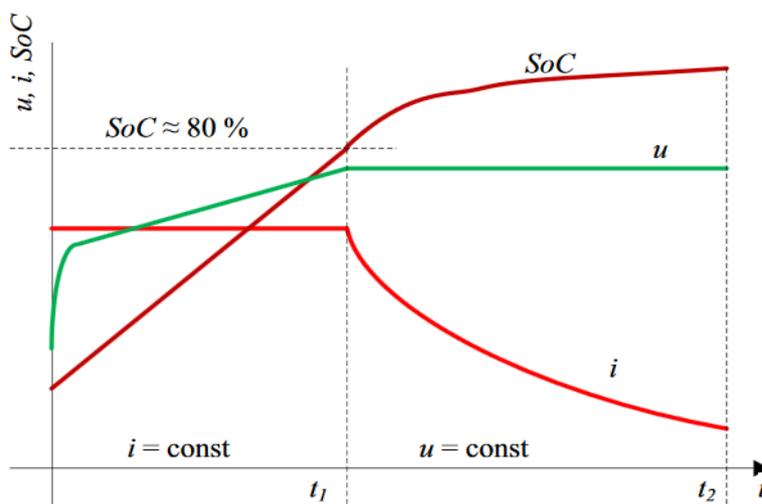

Figure 1: Typical charging curve, where i and u represent the electric current and terminal voltage respectively. (Source Hõimoja et al. (2012))

Although the shape of the charging functions are known, their exact modeling is very complex because it depends on many factors such as: current, voltage, self-recovery and temperature, among others (Wang et al. 2013). The battery state of charge is then often described by differential equations. Since such equations are difficult to embed into optimization algorithms for transportation problems, different approximations are used in the literature. These approximations are presented below compared with real data of a charging function provided by Uhrig et al. (2015). Each of them can be used in a full recharge policy (FR) or in a partial recharge policy (PR).

First segment (FS) : To avoid dealing with the nonlinear segment, Bruglieri et al. (2014) use a linear approximation that considers only the first segment (Figure 2).
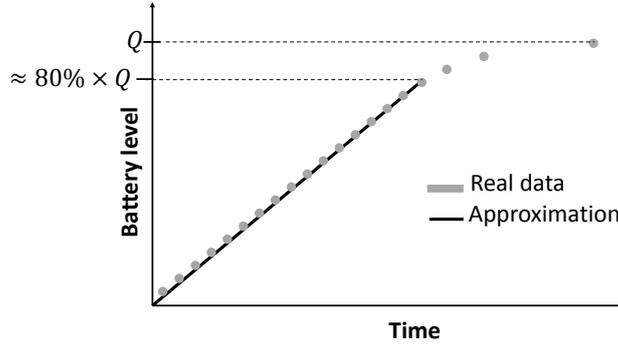
2

Figure 2: First segment approximation (FS)

Linear approximations (L1 and L2) : Although several authors assume a linear approximation (Schneider et al. 2014, Felipe et al. 2014, Sassi et al. 2015, Bruglieri et al. 2015, Desaulniers et al. 2014, Schiffer & Walther 2015, Keskin & Çatay 2016, Szeto & Cheng 2016), they do not explain how the approximation is estimated. Two options can be considered. In the first one (L1) the charging rate of the function corresponds to the slope of the first segment of the piecewise linear approximation (see Figure 3a). This approximation is optimistic, because it assumes that batteries charge up to Q faster than they do in reality. In the second approximation (L2) the charging rate is the slope of the line connecting the first and last observations (see Figure 3b) of the charging curve. This approximation tends to be pessimistic, because over a large portion of the curve, the charging rate is slower than in reality.
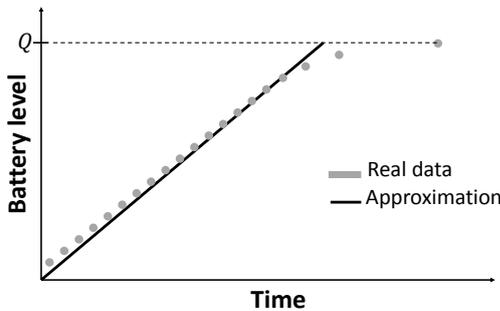
(a) Linear approximation 1 (L1)
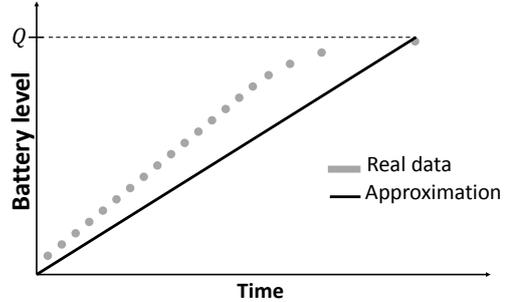
(b) Linear approximation 2 (L2)

Figure 3: Linear approximations of charging functions.

Piecewise linear approximations (PL) : This approximation, proposed by Zündorf (2014) for a shortest path problem with EVs, consists in approximating the charging function by a series of linear segments (see Figure 4a).

In this study, we use the same approximation proposed by Zündorf (2014). To assess the validity of this approximation, we use the data provided by Uhrig et al. (2015). These

authors conducted experiments to estimate the charging time for different charge levels with two types of EVs and three types of charging stations (CSs). We fit piecewise linear functions to the data and obtain approximations with an average relative absolute error of 0.90%, 1.24%, and 1.90% for CSs of 11, 22, and 44 kW, respectively. Figure 4b shows the piecewise linear approximation for a CS i of 22 kW charging an EV equipped with a battery of 16 kWh. In the plot, c_{ik} and a_{ik} represent the charging time and the charge level for the breakpoint $k \in B$ of the CS $i \in F'$, where $B = \{0, .., b\}$ is the set of breakpoints of the piecewise linear approximation.

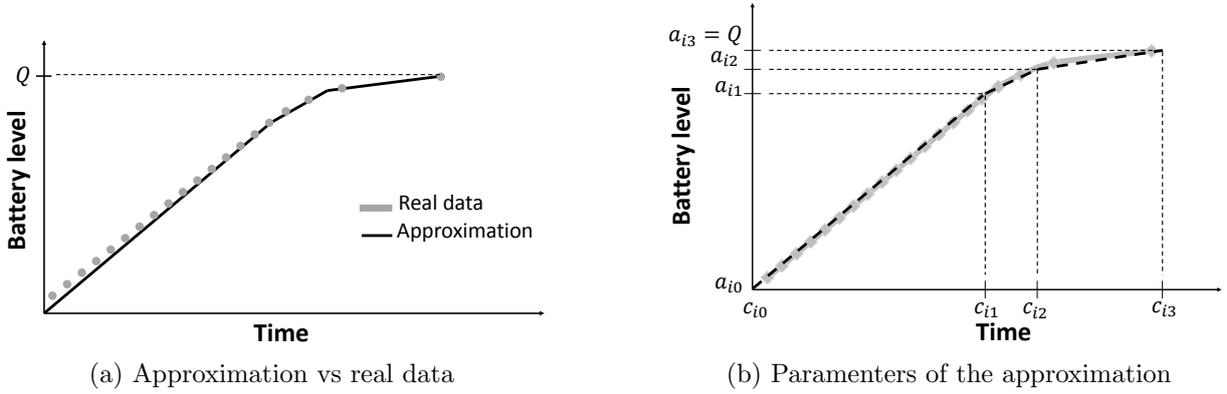(a) Approximation vs real data

(b) Paramenters of the approximation

Figure 4: Piecewise linear approximation (PL).

3. Mixed-integer linear programming formulation

We present in this section the MILP formulation of the eVRP-NL. We also show how it can be adapted to model other approximations and full charging policies

To formulate the eVRP-NL, we introduce the set F' that contains the set F and β copies of each CS (i.e., $|F'| = |F| \times (1 + \beta)$). The value of $1 + \beta$ corresponds to the number of times that each CS can be visited. For this MILP formulation, we use the following decision variables: variable x_{ij} is equal to 1 if an EV travels from vertex i to j, and 0 otherwise. Variables τ_j and y_j track the time and charge level when the EV departs from vertex $j \in V$. Variables q_i and o_i specify the charge levels when an EV arrives at and departs from CS $i \in F'$, and s_i and d_i are the associated charging times (see Figure 5). Variable $\Delta_i = d_i - s_i$ represents the time spent at CS $i \in F'$. Variables z_{ik} and w_{ik} are equal to 1 if the charge level is between $a_{i,k-1}$ and a_{ik}, with $k \in B \setminus \{0\}$, when the EV arrives at and departs from CS $i \in F'$ respectively. Finally, variables α_{ik} and λ_{ik} are the coefficients of the breakpoint $k \in B$ in the piecewise linear approximation, when the EV arrives at and departs from CS $i \in F'$ respectively. The MILP formulation follows:
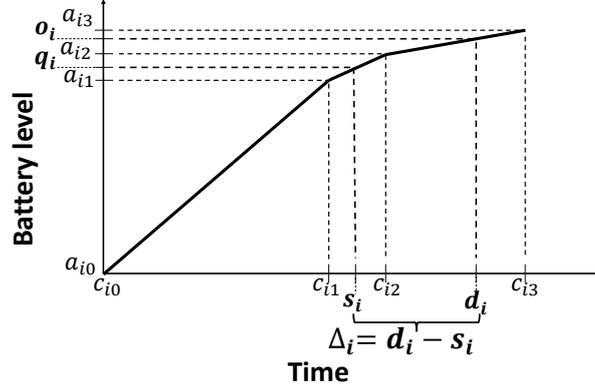
4

Figure 5: Battery charge levels and charging times $i \in F'$

$$\min \sum_{i,j \in V} t_{ij} x_{ij} + \sum_{i \in F'} \Delta_i \tag{1}$$

subject to

$$\sum_{j \in V, i \neq j} x_{ij} = 1, \qquad\qquad \forall i \in I \tag{2}$$

$$\sum_{j \in V, i \neq j} x_{ij} \leq 1, \qquad\qquad \forall i \in F' \tag{3}$$

$$\sum_{j \in V, i \neq j} x_{ji} - \sum_{j \in V, i \neq j} x_{ij} = 0, \qquad\qquad \forall i \in V \tag{4}$$

$$e_{ij} x_{ij} - (1 - x_{ij})Q \leq y_i - y_j \leq e_{ij} x_{ij} + (1 - x_{ij})Q, \qquad \forall i \in V, \forall j \in I \tag{5}$$

$$e_{ij} x_{ij} - (1 - x_{ij})Q \leq y_i - q_j \leq e_{ij} x_{ij} + (1 - x_{ij})Q, \qquad \forall i \in V, \forall j \in F' \tag{6}$$

$$y_i \geq e_{i0} x_{i0}, \qquad\qquad \forall i \in V \tag{7}$$

$$y_i = o_i, \qquad\qquad \forall i \in F' \tag{8}$$

$$y_0 = Q \tag{9}$$

$$q_i \leq o_i, \qquad\qquad \forall i \in F' \tag{10}$$

$$q_i = \sum_{k \in B} \alpha_{ik} a_{ik}, \qquad\qquad \forall i \in F' \tag{11}$$

$$s_i = \sum_{k \in B} \alpha_{ik} c_{ik}, \qquad\qquad \forall i \in F' \tag{12}$$

$$\sum_{k \in B} \alpha_{ik} = \sum_{k \in B} z_{ik}, \qquad\qquad \forall i \in F' \tag{13}$$

$$\sum_{k \in B} z_{ik} = \sum_{j \in V} x_{ij}, \qquad\qquad \forall i \in F' \tag{14}$$

$$\alpha_{ik} \leq z_{ik} + z_{i,k+1}, \qquad\qquad \forall i \in F', \forall k \in B \setminus \{b\} \tag{15}$$

$$\alpha_{ib} \leq z_{ib}, \qquad\qquad \forall i \in F' \tag{16}$$

$$o_i = \sum_{k \in B} \lambda_{ik} a_{ik}, \qquad\qquad \forall i \in F' \tag{17}$$

5

$$d_i = \sum_{k \in B} \lambda_{ik} c_{ik}, \qquad \forall i \in F' \qquad (18)$$

$$\sum_{k \in B} \lambda_{ik} = \sum_{k \in B} w_{ik}, \qquad \forall i \in F' \qquad (19)$$

$$\sum_{k \in B} w_{ik} = \sum_{j \in V} x_{ij}, \qquad \forall i \in F' \qquad (20)$$

$$\lambda_{ik} \leq w_{ik} + w_{i,k+1}, \qquad \forall i \in F', \forall k \in B \setminus \{b\} \qquad (21)$$

$$\lambda_{ib} \leq w_{ib}, \qquad \forall i \in F' \qquad (22)$$

$$\Delta_i = d_i - s_i, \qquad \forall i \in F' \qquad (23)$$

$$\tau_i + (t_{ij} + p_j) x_{ij} - T_{max}(1 - x_{ij}) \leq \tau_j, \qquad \forall i \in V, \forall j \in I \qquad (24)$$

$$\tau_i + \Delta_j + t_{ij} x_{ij} - (S_{max} + T_{max})(1 - x_{ij}) \leq \tau_j, \qquad \forall i \in V, \forall j \in F' \qquad (25)$$

$$\tau_j + t_{j0} \leq T_{max}, \qquad \forall j \in V \qquad (26)$$

$$\tau_0 \leq T_{max} \qquad (27)$$

$$x_{ij} = 0, \qquad \forall i,j \in F' : m_{ij} = 1 \qquad (28)$$

$$\tau_i \geq \tau_j, \qquad \forall i,j \in F' : m_{ij} = 1, j \leq i \qquad (29)$$

$$\tau_j \leq T_{max} \sum_{i \in V} x_{ij}, \qquad \forall j \in F' \qquad (30)$$

$$\sum_{i \in V} x_{ih} \geq \sum_{j \in V} x_{jf}, \qquad \forall h, f \in F' : m_{hf} = 1, h \leq f \qquad (31)$$

$$x_{ij} \in \{0,1\}, \qquad \forall i,j \in V \qquad (32)$$

$$\tau_i \geq 0, y_i \geq 0 \qquad \forall i \in V \qquad (33)$$

$$z_{ik} \in \{0,1\}, w_{ik} \in \{0,1\}, \alpha_{ik} \geq 0, \lambda_{ik} \geq 0, \qquad \forall i \in F', \forall k \in B \qquad (34)$$

$$q_i \geq 0, o_i \geq 0, s_i \geq 0, d_i \geq 0, \Delta_i \geq 0, \qquad \forall i \in F' \qquad (35)$$

The objective function (1) seeks to minimize the total time (travel times plus charging times). Constraints (2) ensure that each customer is visited once. Constraints (3) ensure that each CS is visited at most once. Constraints (4) impose the flow conservation. Constraints (5) and (6) track the battery charge level at each vertex. Constraints (7) ensure that, if the EV travels between a vertex and the depot, it has sufficient energy to reach its destination. Constraints (8) reset the battery tracking to o_i upon departure from CS $i \in F'$. Constraint (9) ensures that the battery charge level is Q at the depot. Constraints (10) couple the charge levels when an EV arrives at and departs from any CS. Constraints (11–16) define the charge level (and its corresponding charging time) when an EV arrives at CS $i \in F'$ (based on the piecewise linear approximation of the charging function). Similarly, constraints (17–22) define the charge level (and its corresponding charging time) when an EV departs from CS $i \in F'$. Constraints (23) define the time spent at any CS. Constraints (24) and (25) track the departure time at each vertex, where $S_{max} = max_{i \in F'}\{c_{ib}\}$. Constraints (26) and (27) ensure that the EVs return to the depot no later than T_{max}. Constraints (28) and (31) avoid the symmetry generated by the copies of the CSs. The parameter m_{ij} is equal to 1 if i and $j \in F'$ represent the same CS. Finally, constraints (32–35) define the domain of the decision variables.

This MILP formulation can be easily adapted to model the other approximations (FS,

L1, and L2) and the different charging policies (FR and PR):

- Full charge and piecewise linear approximations (FR-PL): we replace constraints (17) and (18) by

$$o_i = \sum_{k \in B} \lambda_{ik} a_{ib}, \forall i \in F' \tag{36}$$

$$e_i = \sum_{k \in B} \lambda_{ik} c_{ib}, \forall i \in F' \tag{37}$$

- Partial charge using the first segment (PR-FS): To run our MILP with this assumption, we modify the input data to include only the first segment.

- Partial charge and linear approximations (PR-L): To run our MILP with PR-L1 and PR-L2, we modify the input data so that in the piecewise linear approximation there is a single segment with the corresponding charging rate.

4. Results of the comparison

4.1. Experimental settings

As mentioned in the last section, the MILP formulation uses β copies of the CSs to model multiple visits to the same CS. Although several authors followed this strategy (Conrad & Figliozzi 2011, Erdoğan & Miller-Hooks 2012, Schneider et al. 2014, Sassi et al. 2015, Goeke & Schneider 2015, Hiermann et al. 2016), they do not explain how the value of β is set. It is worth noting that β plays an important role in the definition of the solution space, and therefore it restricts the optimal solution of the model. For instance, an optimal solution found with $\beta = 3$ may not be optimal for $\beta = 4$. In practice, there is no restriction on the number of times that a CS can be visited, but large values of β result in models that are computationally intractable. To overcome this difficulty, we designed an iterative procedure to solve the MILP for increasing values of β. Starting with $\beta = 0$, at each iteration, our procedure (i) tries to solve the MILP to optimality with a time limit of $100\,\mathrm{h}$, and (ii) sets $\beta = \beta + 1$. The procedure stops when the time limit is reached or an iteration ends with a solution s_β satisfying $f(s_\beta) = f(s^*_{\beta-1})$, where $f(\cdot)$ denotes the objective function and $*$ an optimal solution.

4.2. Results

To assess the value of considering partial charging and nonlinear charging function approximations in eVRPs, we conducted an experiment to compare our battery charging assumptions with the assumptions commonly used in the literature. We compare only optimal solutions of the different approaches so that the comparison is independent of the solution method.

Table 1 presents the results. For each charging assumption, we give the objective function value (of), the percentage gap between of and the PR-PL solution (G), the number of routes in the solution (r), and the value of β. Since in practice the charging time is controlled by the nonlinear charging function, the charging decisions of the PR-L solutions are evaluated a posteriori using the piecewise linear approximation. The last rows of Table 1 summarize the results. We present, for each assumption, the average and maximum percentage gap, the number of solutions employing more EVs than in the PR-PL solution, and the number of infeasible solutions.

The results show that solutions based on the full charging policy perform poorly in terms of both objective function (+20.11% on average) and number of routes (8 solutions use a larger fleet) with respect to those based on the partial charging policy. This is because the EVs spend more time than necessary at the CSs. The main motivation for a full charging policy is to avoid complex charging-quantity decisions. However, according to our results, the gain in simplicity does not offset the loss of solution quality.

In the PR-FS assumption EVs can charge their batteries up to only around 80% of the actual capacity. Artificially constraining the capacity may force EVs to detour to CSs more often than necessary when traveling to distant customers. Because the maximum route duration is limited, the time spent detouring and recharging the battery reduces the number of customers that can be visited. Consequently, more routes may be needed to service the same number of customers. Our results confirm this intuition: in 3 of the 20 instances the PR-FS assumption increases the number of routes. Furthermore, in practice some distant customers may not be included in routes unless the EVs can fully use their battery capacity. In our experiments, 9 instances become infeasible under PR-FS. In conclusion, although PR-FS simplifies the problem (avoiding the nonlinear segment of the charging function) it may lead to solutions that are infeasible, or with larger fleets and (on average) 2.70% more expensive.

As mentioned before, PR-L1 assumes that batteries charge faster than they do in reality (Figure 3a). As a consequence, routes based on PR-L1 may in practice need more time to reach the planned charge levels. The extra time may make a route infeasible if there is little slack in the duration constraint. Indeed, a post-hoc evaluation shows that for 14 instances, the PR-L1 solutions are infeasible in practice. On the other hand, PR-L2 assumes that batteries charge slower than in reality (Figure 3b). Overestimating the charging times does not lead to feasibility issues, but the resulting routes may be overly conservative. For instance, in our experiments PR-L2 leads to solutions that are (on average) 1.45% more expensive, and it increases the number of routes in 2 instances.

Table 1: Comparison of our charging assumptions with charging assumptions from the literature

Instance	PR-PL			FR-PL				PR-FS				PR-L1							PR-L2						
												Solution			Evaluation				Solution			Evaluation			
	of	*r*	*β*	*of*	*G(%)*	*r*	*β*	*of*	*G(%)*	*r*	*β*	*of*	*r*	*β*	*of*	*G(%)*	*r*	*β*	*of*	*r*	*β*	*of*	*G(%)*	*r*	*β*
tc0c10s2cf1	**19.75**	3	2	20.82	5.42	3	2	NFS	NFS	NFS	NFS	19.61	3	2	NFE	NFE	NFE	NFE	20.50	3	2	20.22	2.38	3	2
tc0c10s2ct1	**12.30**	2	0	12.53	1.87	2	0	12.61	2.52	3	0	12.22	2	0	12.42	0.98	2	0	12.46	2	0	**12.30**	0.00	2	0
tc0c10s3cf1	**19.75**	3	2	20.82	5.42	3	2	NFS	NFS	NFS	NFS	19.61	3	2	NFE	NFE	NFE	NFE	20.50	3	2	20.22	2.38	3	2
tc0c10s3ct1	**10.80**	2	0	11.10	2.78	2	0	**10.80**	0.00	2	0	10.79	2	0	11.03	2.13	2	0	10.97	2	0	**10.80**	0.00	2	0
tc1c10s2cf2	**9.03**	3	0	9.19	1.77	3	0	**9.03**	0.00	3	0	9.03	3	0	9.12	1.00	3	0	9.14	3	0	**9.03**	0.00	3	0
tc1c10s2cf3	**16.37**	3	2	21.33	30.30	3	2	NFS	NFS	NFS	NFS	15.99	3	1	NFE	NFE	NFE	NFE	16.89	3	2	**16.37**	0.00	3	2
tc1c10s2cf4	**16.10**	3	2	25.31	57.20	4	3	NFS	NFS	NFS	NFS	15.66	3	2	NFE	NFE	NFE	NFE	16.43	3	2	16.23	0.81	3	2
tc1c10s2ct2	**10.75**	3	1	11.14	3.63	3	0	**10.75**	0.00	3	1	10.75	3	0	10.76	0.09	3	0	10.94	3	0	10.78	0.28	3	0
tc1c10s2ct3	**13.17**	2	2	22.76	72.82	3	3	15.98	21.34	3	2	13.06	2	2	NFE	NFE	NFE	NFE	13.60	2	2	**13.17**	0.00	2	2
tc1c10s2ct4	**13.83**	2	1	17.61	27.33	3	1	NFS	NFS	NFS	NFS	13.34	2	1	NFE	NFE	NFE	NFE	14.17	2	1	14.17	2.46	2	1
tc1c10s3cf2	**9.03**	3	0	9.19	1.77	3	0	**9.03**	0.00	3	0	9.03	3	0	9.12	1.00	3	0	9.14	3	0	**9.03**	0.00	3	0
tc1c10s3cf3	**16.37**	3	1	21.33	30.30	3	2	NFS	NFS	NFS	NFS	15.99	3	1	NFE	NFE	NFE	NFE	16.89	3	2	**16.37**	0.00	3	2
tc1c10s3cf4	**14.90**	3	1	18.43	23.69	4	0	NFS	NFS	NFS	NFS	14.56	2	1	NFE	NFE	NFE	NFE	15.18	3	0	15.18	1.88	3	0
tc1c10s3ct2	**9.20**	3	0	11.14	21.09	3	0	**9.20**	0.00	3	0	9.19	3	0	NFE	NFE	NFE	NFE	10.80	3	0	10.57	14.89	3	0
tc1c10s3ct3	**13.02**	2	0	17.06	31.03	3	0	13.07	0.38	2	1	12.98	2	0	13.16	1.08	2	0	13.60	2	0	**13.02**	0.00	2	0
tc1c10s3ct4	**13.21**	2	0	15.54	17.64	3	1	13.58	2.80	3	1	12.92	2	1	NFE	NFE	NFE	NFE	13.71	2	0	**13.21**	0.00	2	0
tc2c10s2cf0	**21.77**	3	3	25.24	15.94	4	2	NFS	NFS	NFS	NFS	14.53	2	2	NFE	NFE	NFE	NFE	22.78	4	4	22.15	1.75	4	4
tc2c10s2ct0	**12.45**	3	2	15.05	20.88	3	3	**12.45**	0.00	3	2	12.44	3	3	NFE	NFE	NFE	NFE	12.93	3	2	**12.45**	0.00	3	2
tc2c10s3cf0	**21.77**	3	2	25.24	15.94	4	2	NFS	NFS	NFS	NFS	14.53	2	2	NFE	NFE	NFE	NFE	23.02	4	3	22.20	1.98	4	3
tc2c10s3ct0	**11.51**	3	0	13.27	15.29	2	0	**11.51**	0.00	3	0	11.50	3	0	NFE	NFE	NFE	NFE	11.92	3	0	11.54	0.26	3	0
Avg. Difference (%)					20.11				2.70							1.04							1.45		
Max. Difference (%)					72.82				21.34							2.13							14.89		
Solutions with larger fleet						8				3							0								2
Infeasible solutions	0				9								14							0					

NFS: Non-feasible solution, NFE: Non-feasible evaluation
$G(\%) = (of - of_{PR-PL})/of_{PR-PL} \times 100$

References

Bruglieri, M., Colorni, A. & Luè, A. (2014), 'The vehicle relocation problem for the one-way electric vehicle sharing: An application to the Milan case', *Procedia - Social and Behavioral Sciences* **111**, 18 – 27.

Bruglieri, M., Pezzella, F., Pisacane, O. & Suraci, S. (2015), 'A variable neighborhood search branching for the electric vehicle routing problem with time windows', *Electronic Notes in Discrete Mathematics* **47**, 221–228.

Conrad, R. G. & Figliozzi, M. A. (2011), The recharging vehicle routing problem, *in* T. Doolen & E. V. Aken, eds, 'Proceedings of the 2011 Industrial Engineering Research Conference', Reno, NV, USA.

Desaulniers, G., Errico, F., Irnich, S. & Schneider, M. (2014), Exact algorithms for electric vehicle-routing problems with time windows, Technical report, GERAD, G-2014-110.

Erdoğan, S. & Miller-Hooks, E. (2012), 'A green vehicle routing problem', *Transportation Research Part E: Logistics and Transportation Review* **48**(1), 100–114.

Felipe, A., Ortuño, M. T., Righini, G. & Tirado, G. (2014), 'A heuristic approach for the green vehicle routing problem with multiple technologies and partial recharges', *Transportation Research Part E: Logistics and Transportation Review* **71**, 111 – 128.

Goeke, D. & Schneider, M. (2015), 'Routing a mixed fleet of electric and conventional vehicles', *European Journal of Operational Research* **245**(1), 81 – 99.

Hiermann, G., Puchinger, J., Ropke, S. & Hartl, R. F. (2016), 'The electric fleet size and mix vehicle routing problem with time windows and recharging stations', *European Journal of Operational Research* **252**(3), 995 –1018.

Hõimoja, H., Rufer, A., Dziechciaruk, G. & Vezzini, A. (2012), An ultrafast ev charging station demonstrator, *in* 'Power Electronics, Electrical Drives, Automation and Motion (SPEEDAM), 2012 International Symposium on', IEEE, pp. 1390–1395.

Keskin, M. & Çatay, B. (2016), 'Partial recharge strategies for the electric vehicle routing problem with time windows', *Transportation Research Part C: Emerging Technologies* **65**, 111 – 127.

Pelletier, S., Jabali, O., Laporte, G. & Veneroni, M. (2015), Goods distribution with electric vehicles: Battery degradation and behaviour modeling, Technical report, CIRRELT-2015-43.

Sassi, O., Cherif-Khettaf, W. & Oulamara, A. (2015), Iterated tabu search for the mix fleet vehicle routing problem with heterogenous electric vehicles, *in* H. A. Le Thi, T. Pham Dinh & N. T. Nguyen, eds, 'Modelling, Computation and Optimization in Information Systems and Management Sciences', Vol. 359 of *Advances in Intelligent Systems and Computing*, Springer International Publishing, pp. 57–68.

Schiffer, M. & Walther, G. (2015), The electric location routing problem with time windows and partial recharging, Technical report, RWTH Aachen University.

Schneider, M., Stenger, A. & Goeke, D. (2014), 'The electric vehicle-routing problem with time windows and recharging stations', *Transportation Science* **48**(4), 500–520.

Szeto, W. & Cheng, Y. (2016), Artificial bee colony approach to solving the electric vehicle routing problem, *in* 'Annual Meeting of the Transportation Research Board, TRB 2016'.

Uhrig, M., Weiß, L., Suriyah, M. & Leibfried, T. (2015), E-mobility in car parks–guidelines for charging infrastructure expansion planning and operation based on stochastic simulations, *in* 'the 28th International Electric Vehicle Symposium and Exhibition, KINTEX, Korea'.

Wang, H., Liu, Y., Fu, H. & Li, G. (2013), 'Estimation of state of charge of batteries for electric vehicles', *International Journal of Control and Automation* **6**(2), 185–194.

Zündorf, T. (2014), Electric vehicle routing with realistic recharging models, Master's thesis, Karlsruhe Institute of Technology, Karlsruhe, Germany.